Published in final edited form as:

SAE Int J Engines. 2018 ; 11(6): 1273–1305. doi:10.4271/2018-01-0319.

Benchmarking a 2016 Honda Civic 1.5-liter L15B7 Turbocharged Engine and Evaluating the Future Efficiency Potential of Turbocharged Engines

Mark Stuhldreher, **John Kargul**, **Daniel Barba**, **Joseph McDonald**, **Stanislav Bohac**, **Paul Dekraker**, and **Andrew Moskalik**

U.S. Environmental Protection Agency

Abstract

As part of the U.S. Environmental Protection Agency's (EPA's) continuing assessment of advanced light-duty automotive technologies to support the setting of appropriate national greenhouse gas standards and to evaluate the impact of new technologies on in- use emissions, a 2016 Honda Civic with a 4-cylinder 1.5-liter L15B7 turbocharged engine and continuously variable transmission (CVT) was benchmarked. The test method involved installing the engine and its CVT in an engine dynamometer test cell with the engine wiring harness tethered to its vehicle parked outside the test cell. Engine and transmission torque, fuel flow, key engine temperatures and pressures, and onboard diagnostics (OBD)/CAN bus data were recorded.

This paper documents the test results for idle, low, medium and high load engine operation, as well as motoring torque, wide-open throttle torque and fuel consumption during transient operation using both EPA Tier 2 and Tier 3 test fuels. Particular attention is given to characterizing enrichment control during high load engine operation. Results are used to create complete engine fuel consumption and efficiency maps and estimate CO2 emissions using EPA's ALPHA full vehicle simulation model, over regulatory drive cycles. The design and performance of the 1.5-liter Honda engine are compared to several other past, present, and future downsized-boosted engines and potential advancements are evaluated.

Introduction/Background

The National Center for Advanced Technology (NCAT), part of EPA's National Vehicle and Fuel Emissions Laboratory (NVFEL) in Ann Arbor, Michigan, leads a team that assesses the effectiveness of advanced low emission and low fuel consumption technologies by benchmarking a broad range of key light-duty vehicles, engines and transmissions. The NCAT team benchmarks advanced technologies using laboratory test methods to characterize engine controls and fuel consumption. Technologies benchmarked thus far include boosted and high compression ratio naturally-aspirated engines (containing advanced components such as variable valve lift and timing, cylinder deactivation and

Contact Information Mark Stuhldreher, National Center for Advanced Technology, US EPA – National Vehicle and Fuel Emissions Laboratory, 734-214-4922, Stuhldreher.mark@epa.gov.

integrated exhaust manifolds), high-ratio 8+ gear automatic transmissions, continuous variable transmissions, and hybrid components.

NCAT leverages in-depth, detailed engineering analyses along with extensive engine and chassis dynamometer laboratory testing to evaluate advanced vehicle, engine and transmission technology. The test data are used for a variety of purposes, including documenting engine performance in complete engine maps, performing technical analyses regarding technology effectiveness, and providing information for full vehicle simulations with EPA's Advanced Light- Duty Powertrain and Hybrid Analysis (ALPHA) tool [1]. Both laboratory test data and ALPHA simulation results continue to be used to support evaluation of light-duty vehicle fuel economy and greenhouse gas emissions standards and are also being used to evaluate the gap between laboratory and actual in-use emissions.

Downsized boosted engines are a key technology being used today to meet performance targets as well as GHG and fuel economy standards. To understand the current performance and efficiency of boosted engines on the frontier of automotive development, EPA benchmarked a 2016 Honda Civic with a 4-cylinder 1.5-liter L15B7 turbocharged engine and its CVT. The complete benchmarking study of this vehicle included both chassis testing and engine dynamometer testing to measure vehicle and engine efficiencies. The paper focuses on the following topics:

1. **Benchmarking Method** - The benchmark testing involved installing the engine in an engine dynamometer test cell with the engine wiring harness tethered to the complete vehicle parked outside the test cell. This technique enabled the engine to be mapped using the vehicle's stock engine control unit (ECU) with its as-built calibrations along with all the needed input signals, including those integrated with other vehicle sensors. The data measured include torque, fuel flow, temperatures, pressures, in-cylinder pressure, and onboard diagnostics (OBD)/ CAN bus data.
2. **Test Data Collection and Analysis** - Engine data were collected using both steady-state and transient test procedures to appropriately characterize engine operation at idle, low/mid and high loads. At the higher loads, a transient test procedure was created to observe the changing control and performance of the engine that often occurs when the ECU begins to protect the engine from excessive temperatures, pre-ignition and knock. While vehicles rarely operate in the high load region of their engine map over the city and highway regulatory cycles, engine emissions can increase significantly during off-cycle, real-world driving and have become an increasingly important area of research at EPA and in the automotive industry.
3. **Fuel Consumption Maps** - After the engine benchmark testing was completed, the engine fuel efficiency maps were generated from the engine test data. These maps are needed as inputs to ALPHA, EPA's full vehicle simulation model, to estimate CO_2 emissions over the regulatory city and highway drive cycles.
4. **Comparison of the Honda Engine to Other Production Engines Using ALPHA** - To produce analytical CO2 emission results, EPA used ALPHA, a

physics-based computer simulation model capable of analyzing various vehicle types and powertrain technologies. To simulate drive cycle performance, the ALPHA model requires various vehicle parameters as inputs, including vehicle inertia and road load coefficients, component efficiencies, and vehicle operation data [2].

5. **Technology Comparison with Other Turbo Engines** - A comparative assessment of the design and performance of the 1.5-liter Honda L15B7 engine technologies against several other past, present, and future downsized-boosted engines was conducted. This analysis helped to demonstrate how Honda's new boosted engine fits into the technology frontier with other boosted engines being developed today. The analysis examined which technologies that are being developed are used by this engine and whether there is potential to add additional technologies to make the engine even more efficient.

6. **Potential for Improving Efficiency** - Finally, two examples of potential future technology advancements that could extend the CO2 reduction benefits of turbocharged engines are discussed.

1. Benchmarking Method

EPA's method for benchmarking an engine involved installing the engine in an engine dynamometer test cell while connecting (tethering) the engine's wiring harness to the complete vehicle, which is parked adjacent to the test cell. This testing technique enables the engine to be operated using the vehicle's stock engine control unit (ECU) with its as-built calibrations along with all the needed input signals including those integrated with other vehicle sensors.

Description of Test Article

The engine used in this project was a 2016 Honda Civic 1.5-liter L15B7 engine, which is a turbocharged, direct-injection gasoline engine with side-mounted injection that operates at a maximum pressure of 200 bar [3]. The engine was tethered to its vehicle located outside the engine test cell to make use of the stock engine and vehicle controllers. Table 1 summarizes information that identifies the vehicle system used in this test program.

Testing was performed in a light-duty engine dynamometer test cell located at the National Vehicle and Fuel Emissions Laboratory (NVFEL) in Ann Arbor, Michigan. The test cell equipment and instrumentation are listed in Table 2.

Data Collection Systems

Test cell data acquisition and dynamometer control were performed by iTest, a software package developed by A&D Technology, Inc., Combustion data were analyzed by an MTS Combustion Analysis System (CAS). RPECS-IV (Rapid Prototyping Electronic Control System - IV) is supplemental data acquisition software developed by Southwest Research Institute (SwRI). RPECS directly measures and logs ECU input/output (I/O) along with test

cell data. Temperatures, pressures, and test cell data were sent from iTest to RPECS via CAN. The engine control and analysis systems are summarized in Table 3.

Vehicle Tethering

The objective of this benchmarking was to characterize the engine while operating in an engine dynamometer test cell as though it were operating in the vehicle. The ECU in today's vehicles requires communication with other control modules to monitor the entire vehicle's operation (security, entry, key on, dashboard signals, etc.). Because the ECU needs signals from these modules to operate, the signals need to be extended to the test cell so the ECU can receive signals indicating correct vehicle operation. For this benchmark testing, the wiring harnesses were lengthened connecting the ECU in the test cell to the rest of the vehicle. As a result, the engine located in the dynamometer cell was then tethered to its vehicle chassis located outside the cell. Figure 1 illustrates the tethered wiring harness. Wires were tapped into for all the signals from the ECU to the engine so the signals could be monitored.

Engine Configuration

Figure 2 illustrates the engine configuration and sensor location in the dynamometer test cell. The sensor colors shown in the upper left corner of the figure indicate which systems are monitored.

The stock engine systems were used with the addition of instrumentation as follows:

- *Intake*: The stock air box and plumbing were used with a laminar flow element (LFE) connected to the air box inlet.
- *Exhaust*: The stock exhaust system was used including catalyst and mufflers (Figure 2 shows only one muffler). The exhaust system outlet is connected to the constant volume sampling system (CVS) dilution tunnel via 2-inch diameter tubing. Emission tunnel pressure was controlled to approximately P^{atm} ±1.2 kPa, which is a variation of pressure well below the required limits specified within the U.S. Code of Federal Regulations for chassis dynamometer testing [5].
- *Cooling system*: The stock cooling system was used, but the radiator was replaced with a cooling tower. The stock engine thermostat was used to control engine coolant temperature. The Honda Civic was chassis tested before the engine was benchmark tested and the engine coolant temperatures were observed for these tests and used as guide for the coolant temperature set point [6]. The cooling tower was controlled to 85°C by the test cell control system.
- *Oil system*: The stock oil cooler was connected to a chilled water system and controlled to 90°C by the test cell control system.
- *Charge air cooling*: During testing, engine temperatures were maintained to a level representative of real-world use, where the engine would be cooled by airflow into the engine compartment as vehicle speed increases. Real-world testing of the 2016 Honda Civic identified 30–40°C as the target intercooler air temperature range for the engine. In the test cell, air charge temperature was

maintained at 30 to 40°C by using the stock intercooler sandwiched to a water-to-air heat exchanger and fans. The actual temperature for each sampled data point is recorded with each data point.

- *Front End Accessory Drive (FEAD)*: The stock belt and pulley FEAD system was used.
- *Alternator*: The alternator was modified for no electrical output by removing the field coils.
- *Fuel*: The engine tests were performed with the EPA Certification Tier 2 and Tier 3 fuels shown in Table 4.

Engine-Dynamometer Setup

To gather data for this benchmarking program, two methods of coupling the engine to the dynamometer were needed. Direct drive shaft engine to dynamometer coupling worked best to gather most of the data. However, when idling and operating in the low rpm region of the engine's operating map (especially below 1000 rpm), the high torsional stiffness of the rigid driveshaft tends to create excessive torque fluctuations not present when the engine operates in a vehicle. Consequently, a second method of coupling the engine to the dynamometer through its transmission (a CVT) and torque converter was used for gathering data where the torque measurement is very sensitive to the engine's torsional accelerations.

Setup without the CVT -—In this method, the engine was coupled to the dynamometer via the drive shaft and by using a stripped-down Honda manual transmission housing with its flywheel and clutch, a combination which was available from a Honda Civic with a 1.8 L engine. This transmission housing was modified by removing all the internal gear sets and incorporating a single through shaft. The flywheel from the Honda 1.8 L engine has the same crankshaft bolt pattern as the flywheel for the new 1.5-liter engine.

A single torque sensor from HBM was mounted in line between the transmission and dynamometer. The transmission's clutch disk with torsional spring assembly and rubber isolated driveshaft results in stable torque measurements. This setup allowed the engine to be started using its starter, to be full-load tested, and to be declutched for unloaded engine idling. This setup was used from 1000 to 5000 rpm.

Setup with the CVT -—In this method, the engine was coupled to the dynamometer via drive shaft and through the Honda Civic's CVT and torque converter with torque sensors before and after the CVT (shown in Figure 3).

During this part of this setup for the engine benchmarking, the CVT torque converter lock-up solenoid was controlled remotely, allowing the torque converter clutch to be unlocked, enabling low speed operation with minimal torsional stiffness. This engine-CVT setup also enabled idling measurements with transmission in park, neutral, or drive, with the torque converter locked or unlocked, and with the CVT output shaft locked or unlocked. Measurements under these various conditions accurately replicate how the engine operates in a vehicle that is decelerating or is not moving.

Special consideration for measuring torque -—Special care is required for measuring engine torque and for measurements from other sensors that are sensitive to engine cyclical dynamics. These signals become more sensitive when mounting the torque sensor between the engine and CVT as required for the engine setup used for testing in the idle-to-low-load region discussed in the next sub-section and shown in Figure 5. When these sensors are sampled in a time domain at 100 Hz, signal aliasing occurs and distorts the reported signal values.

These sensors cannot be correctly sampled at 100 Hz but rather must be sampled in the engine crank angle domain. The method consists of sampling the torque sensor output voltage with a high-speed data acquisition system, in this case RPECS, and averaging the samples over one engine cycle. The averaged value is then logged to iTest. An example torque signal aliasing of the time sampled method is shown in Figure 4. This graph was generated by logging a load sweep over 60 seconds and shows both the same torque signals, one sampled in the crank angle domain (CAD) and the other sampled in the time domain.

2. Test Data Collection and Analysis

Both steady-state and transient engine test data are collected during the benchmark testing. Two different test procedures were needed to appropriately replicate steady-state engine operation at low/mid loads and transient engine operation at high loads. Before proceeding further, it is important to grasp a view of all the steady-state and transient test data points gathered in the three load regions during the EPA benchmarking process, highlighted in Figure 5.

The test data points (black dots in Figure 5) in the low-mid load region were collected using straightforward steady-state procedures that have previously been described by EPA in SAE papers related to engine benchmarking [6, 7, 8]. These points are below the region where enrichment was first observed in this benchmarking program. These points generally have stable and consistent engine controls (e.g., spark timing, valve timing, start of injection), allow the use of relatively slow response fuel flow measurement systems over a 30- second data collection window, and are therefore straightforward to analyze and report. Complete data packages from previous EPA benchmarking are publicly available on a test data website [9, 10, 11]. At time of publishing this paper, the complete data package for the Honda engine will be available through EPA's testing website: (https://www.epa.gov/vehicle-and-fuel-emissions-testing/science- and-technology-development-national-vehicle-and-fuel).

High load operating points (blue triangles and green squares in the high load region in Figure 5) are defined in this paper as the region where enrichment is observed. In this region, data cannot be collected with steady-state procedures due to the transient nature of the engine control, which is employed to protect the engine from excessively high temperatures, to avoid pre-ignition at low speed/high load, or to avoid knock at high speed/high load. The ECU avoids these damaging effects by transiently adjusting the engine control parameters, often at the expense of fuel consumption and efficiency, through control techniques such as spark retard and fuel enrichment.

To properly benchmark the engine and monitor its changing control and performance in the high load region, a transient test procedure is required. Characterization of the transient behavior of the engine at high load is most important when creating engine fuel maps that can be used to estimate "off-cycle" emissions. Off-cycle emissions occur when the vehicle is operated above power levels needed over the basic GHG regulatory certification cycles (city/FTP, highway/HWFET). This type of testing and modeling of more extreme operation sometimes experienced in real world driving (including the use of more aggressive regulatory cycles such as the US06) is an increasingly important area of research at EPA and in the wider automotive community. While most vehicles rarely operate under such sustained high load conditions, when they do operate at high load, emissions can be orders of magnitude higher and can be a significant contributor to in-use emissions.

Test data for engine operation at low speeds at or near idle conditions (red × and orange + in Figure 5) cannot be collected acceptably with the direct coupling arrangement of the engine to the dynamometer typically used for mid and high load testing due to the high torsional stiffness of the driveshaft and high rotational inertia of the dynamometer. Gathering data in the low speed/low torque area of the engine map is accomplished by incorporating a transmission (CVT or automatic) into the test setup producing driveline behavior similar to the behavior found in the vehicle.

Benchmarking Details

To gather the complete set of test data shown in Figure 5, the engine was operated with and without the CVT in the three key phases identified in Table 5. Each different phase is discussed in more detail to explain how each of the various types of data were measured and processed to develop a complete fuel efficiency map suitable for use in a full vehicle simulation model such as ALPHA.

Data points for the low-mid load region (black dots in Figure 5) are typically collected first during the engine benchmarking process because these samples help assure that the engine is set up correctly with no unexpected resonance frequencies, operating within acceptable temperature ranges, and is tethered appropriately so that the OBD II (on board diagnostics phase-II) system is not showing current or pending malfunction codes. Engine-dynamometer setup for this portion of the benchmarking is faster since the transmission of the vehicle is not yet needed.

Engine Operation ——For this phase of testing the engine is operated using a test procedure to appropriate characterize steady-state engine operation at low/mid loads. The core of the steady-state engine map contains the primary operating range of the engine, which is characterized by closed-loop fuel control/stoichiometric operation and spark timing that allows combustion phasing that will result in best efficiency. The stability and repeatability of engine operation in this load region allows for straightforward collection of steady-state measurements on an engine dynamometer.

Data Collection ——Engine operation consists of holding the engine at a fixed speed (with the engine dynamometer) for approximately 30 seconds, on average, by commanding a fixed pedal position. Operation at this point is held until the engine torque, fuel flow, and exhaust

temperature stabilize. The data are then logged for 10 seconds at 10 Hertz sampling and averaged by using iTest. For each engine speed, the sequencing procedure steps through an array of pedal commands from low to high (0 to 100% pedal position) and records the steady-state data for each test point. The engine speed is then incremented to the next highest rpm and the torque array is repeated. Generally, mapping points are denser in the lower engine speeds and load areas of operation.

While this engine did not consume fuel at all of the zero pedal test points, an accurate measurement of torque is necessary to ensure an appropriate amount of drag is placed on the drivetrain during simulation of coasting conditions. These data are gathered to determine the energy consumed during coasting, which would not be energy that would be available to be captured in a vehicle featuring a hybrid powertrain or alternator regeneration technology such as Mazda's i-ELoop [12].

Data points for the high load region are gathered in this phase of the benchmarking. This operation pushes the engine to operate at its highest torque levels across all engine speeds. No CVT is used in the engine-dynamometer setup for this phase of benchmark testing.

When operating in high load conditions, the engine ECU controls several parameters such as A/F ratio and spark timing differently depending upon speed and load on the upper limits of the engine performance. Generally, engines operate at a stable stoichiometric A/F ratio from idle to approximately 70% load. Above 70% load, the engine ECU will transition the A/F ratio from stoichiometric to enriched as needed to protect the engine from excessive heat, pre- ignition and knock.

Engine Operation -—For this phase of testing, the engine is operated at high loads near and including wide-open throttle (WOT) using a special test procedure to activate the transient response that occurs when the engine is protecting itself at high loads. While EPA has successfully used a sweep test (where the accelerator pedal is set to WOT and the engine speed is swept from low to high rpm), in some previous test programs of naturally aspirated and turbocharged gasoline engines to determine the maximum torque curve for use in simulations, we have found that sweep tests often underpredict the maximum achievable torque of the engine. This is primarily due to the high temperatures resulting from the relatively slow rpm sweep (5–10 seconds) and the subsequent de-rating due to engine protection controls. For this reason, EPA prefers to run a high load transient procedure to determine WOT conditions, and to use the sweep test to better understand protection controls and to potentially fill in some data gaps for the lower speed range of the WOT curve.

The minimum high load points are identified during the steady-state testing done in Test Phase 1, when the A/F ratio is found to change from stoichiometric to enriched during its stability and steady-state logging time period of approximately 30 seconds. For each transient test point, the accelerator pedal is held at approximately 1/3 load, and the engine is allowed to stabilize. Then, the accelerator pedal is ramped to the desired torque for the test point in approximately one second (this portion of the test has come to be called the "stab test"). This engine operating condition is maintained until a time limit is reached (generally

approximately 20 seconds worth of data is collected). The engine is stepped through an array of speed and load points in a sequence similar to the steady-state procedure.

Data Collection ——For each data point, the data are logged continuously at 100 Hz while the engine torque is ramping up to the desired torque value and while operation is held at that point for 30 seconds. The data are then post-processed to determine the peak torque, final torque, transition time from stoichiometric to enriched, brake thermal efficiency (BTE), and other key engine criteria. A graphic example of a transient data set is shown in Figure 6. The exhaust lambda data is acquired from an air-fuel ratio analyzer manufactured by ECM (located in Los Altos, California). The analyzer contains a wideband oxygen sensor which is operated per factory suggested settings.

Special Post-Processing necessary for Transient Data Points -—Once the roughly 30 seconds of transient data have been collected for all of the high load points, the captured data streams must be post- processed to determine the specific final results. These results will be used later on to develop brake-specific fuel consumption (BSFC) and BTE maps suitable for use in vehicle simulation models.

The basic calculations for transient data points include a straightforward averaging of a number of repeated measurements. However, before the averaging can be done for these transient points, the data set for each data point must be analyzed to determine the two specific time intervals that occur when the engine is at or near its high load operating torque. These two time intervals occur at approximately the time the engine transitions from stoichiometric to fuel-enriched operation. The yellow torque line in the top chart of Figure 7 illustrates the change in engine torque that occurs after the torque achieves ~200 N-m due to the transition to enriched operation. The blue line in the bottom chart in Figure 7 shows the change in exhaust lambda (air-fuel equivalence ratio).

Initial and Final Intervals: To characterize the high load region of operation, EPA's goal was to define an initial time window after the target high load torque is achieved, while the engine is still in stoichiometric operation, and then a final time window after control stabilizes to a long term steady-state value in enriched operation. Once the two intervals are determined, then post-processing computes the straightforward average of the measurements in the interval.

The average values in these two intervals bookend operation in the high load region. The "Initial" high load interval (violet highlighted timeframe in Figure 7) contains the stable torque and fuel consumption data measurements representing how the engine operates when it stays at that data point for only a short period of time. The criteria to select the initial interval begin with defining the time when the engine first achieves a stable torque condition. The initial high load interval ends when torque (yellow signal in top chart) becomes unstable (a period of time after the engine's spark begins to retard and lambda drops significantly below unity as shown in bottom chart).

The "Final" high load interval (green highlighted timeframe in Figure 7) contains the stable torque and fuel consumption data measurements representing how the engine operates when

it stays at that high load data point for a sustained period of time. The final high load interval begins when torque becomes stable again, and ends at the end of the data point's sample.

Special measurement of fuel consumption during transient operation: Typically, when benchmarking an engine, steady-state operation allows for the straightforward measurement of fuel consumption either by a fuel flow meter or by exhaust emissions. EPA generally uses a fuel flow meter when benchmarking engines. Due to transport lag and other time delays, these two measurement techniques are unable to accurately quantify the amounts of fuel consumed over short periods of engine operation. Consequently, EPA uses a third technique that uses fuel injector data to measure how much fuel is consumed.

By capturing detailed measurements of fuel injector pulse duration and fuel rail pressure during steady-state testing, an injector calibration can be constructed to then estimate fuel consumption. For improved accuracy, the fuel rail pressure is measured via a high speed data acquisition system, synchronously with the crankshaft to minimize the distortion caused by rapid fluctuations in pressure. The textbox labeled "Injector Fuel Flow Correlation" explains the method of injector fuel flow correlation that was developed for this study.

The red and blue fuel flow lines superimposed in the middle chart in Figure 7 represent the fuel flow from the meter and the fuel flow calculated from the engine's fuel injectors, respectively. Post- processing the average fuel consumption for each data point uses fuel meter values, unless those instantaneous readings become unstable, at which point the processor substitutes injector measurements to compute the average.

Figure 9 shows a summary of how exhaust lambda changes between these initial and final intervals.

The steady-state average torque, speed and fuel flow points, shown previously as black dots in Figure 5, were combined with the average initial and final transient torque data, shown previously as blue triangles and green squares in Figure 5, to generate base contour maps such as exhaust lambda and BTE.

The top chart in Figure 10 illustrates the BTE map using the high load "initial" torque data points (blue triangles). The bottom chart in Figure 10 illustrates the BTE map using the high load "final" torque data points (green triangles).

Since the ALPHA model computes combined vehicle CO2 and fuel consumption using the light- to moderate-load regulatory city and highway drive cycles, EPA uses data from the initial interval when subsequently building the complete engine maps for use in ALPHA vehicle simulations.

Appendix A contains larger versions of these charts along with other key benchmarking data: BSFC, BTE, exhaust lambda, compression ratio, exhaust camshaft phasing, intake camshaft phasing, Atkinson ratio[1], spark timing, and valve overlap. In addition, complete

[1]For this study, Atkinson Ratio is the ratio of effective expansion stroke length to effective compression stroke length, where the extremity of each stroke is determined by the location corresponding to 1mm of valve opening.

BSFC and BTE maps generated from the engine benchmarking data and/or other sources by extrapolating over the full range of engine speed and load (discussed in the next section) are included in Appendix A.

Data points for the idle-low load region of engine operation shown in Figure 5 are gathered in this final phase of the engine benchmarking. As mentioned earlier in the engine-dynamometer setup section, collecting steady-state data on engine operation at or near idle conditions on a dynamometer has a few challenges. Coupling the engine with its torque converter is necessary while the engine is at or near idle because the engine is more sensitive to torsional accelerations. Typical coupling of the engine and dynamometer using a traditional driveshaft results in a high torsional stiffness and high rotational inertia at idle relative to what would be experienced in a vehicle with an open clutch or unlocked torque converter. The resulting configuration tends to not replicate in-vehicle engine operation as these factors can interact with the engine control logic leading to instability within the idle speed control or false positive detection of misfire events due to issues with measuring crankshaft acceleration.

To accommodate these issues, data in the low speed and low torque areas of the engine map which are sensitive to this torsional stiffness were gathered through a different test setup. To connect to Honda's torque converter, the engine was simply coupled to the complete CVT from a 2016 Honda Civic.

Engine Operation: Testing in the idle-low load region is done in two parts. In the first part of the idle-low load testing, steady-state engine-CVT operation consists of controlling the engine speed/torque settings using a pedal sweep with the CVT shift mechanism in neutral with the CVT output shaft held at zero rpm by the dynamometer. The torque converter is unlocked as controlled by the ECU. The first data point of this sweep represents the engine's idle point (pedal equal zero) with CVT in neutral. Increasing the pedal steps through an array of points as shown by the orange + points in Figure 11 and in Figure 5.

In the second part of idle-low load testing, the steady-state engine- CVT operation consists of controlling the engine speed/torque settings using a pedal sweep with the CVT shift mechanism in drive and with the CVT output shaft held at zero rpm by the dynamometer. The torque converter is unlocked as controlled by the ECU. The first data point of this sweep represents the engine's idle point (pedal equal zero) with CVT in neutral. Increasing the pedal steps through an array of points is shown by the red "x" points in Figure 11 and in Figure 5.

Data Collection ——The test procedures for testing this region require the engine operation at each point the pedal position is held until the engine torque, fuel flow, and exhaust temperature stabilize for approximately 30 seconds before a 15 to 30 second window of data is collected at 10 Hertz and averaged.

3. Fuel Consumption Maps

Once the benchmarking data has been gathered, it must be processed into a form suitable to estimate CO_2 emissions over the regulatory drive cycles. In support of this work, the NCAT team developed techniques to combine the engine operating test data into a set of complete engine maps suitable for use in vehicle simulation models like ALPHA and other technical analyses [13]. These complete engine maps estimate the fuel consumption of an engine over its complete operating range, spanning idle and motoring, wide-open- throttle and the pre-defined maximum "redline" engine speed. For each engine to be simulated within ALPHA, NCAT uses an in-house modeling tool to combine engine test data from its benchmarking tests and/or from other sources like technical papers and conference presentations into consistent, publishable "complete" maps.

Fuel Efficiency Map on Tier 2 Fuel

Figure 12 shows the BTE map generated from EPA's benchmarking of the 2016 Honda 1.5-liter L15B7 engine when running on Tier 2 certification fuel. The "initial" transient high load data (rather than the "final" transient high load data) were used along with the steady-state low mid and idle low load data to generate the complete ALPHA engine maps, since the two-cycle regulatory procedure [Federal Test Procedure (FTP) and Highway Fuel Economy Test (HWFET)] do not operate at the high load data points very often or long enough at any one point for the engine to transition to rich operation.

This engine was also mapped using Tier 3 Certification fuel and the mapping show very similar BTE results. While the focus of the paper is on the engine's performance using the Tier 2 fuel currently used for compliance with U.S light-duty GHG standards, Appendix B contains a brief comparison of some of the efficiency test data from engine mapping with both Tier 2 and Tier 3 fuels.

Comparison of EPA's Benchmarking Engine Map to Honda's Published Map

Before EPA completed its benchmarking of the Honda 1.5-liter L15B7 engine, Honda published two maps representative of the engine, one with their SAE paper [4] and another from Honda's poster presentation at the 2016 SAE World Congress Exhibition. Both of their maps are shown in Figure 13. As a point of reference to compare to EPA's recently completed benchmarking-based map, Figure 14 presents the BTE map generated by EPA from Honda's published image from the SAE World Congress shown on the right within Figure 13. Of necessity, the map generated by EPA in Figure 14 includes estimations that extend beyond the data provided in Honda's image, which ranged from 1000 rpm to 4000 rpm, and from 20 Nm to 205 Nm (shown as the black dashed object in Figure 14 and Figure 15). Reference [13] discusses how EPA works with published engine images to create engine fuel maps suitable for vehicle simulation.

Figure 15 is a plot showing the difference between BTE in Figure 14 (calculated by EPA from Honda's published BSFC map in Figure 13) and the BTE map based on EPA's benchmarking data (Figure 12).

As discussed by Dekraker, [13] published maps are an excellent resource for quickly incorporating the latest cutting edge technologies into ALPHA, often well before benchmark testing can be performed on the actual production engine. However, some caution is needed when using data in published maps because these map images often lack accompanying descriptions of how the data were collected, how the map was generated, and what changes might be needed when integrating the engine into a production vehicle (e.g., mitigating noise, vibration, harshness (NVH), adjusting calibrations to meet emissions standards that differ depending on market, etc.).

In addition, Honda's published maps spanned only 1000 rpm to 4000 rpm, did not include data below 20 Nm, and were either clipped or uncertain above approximately 205 Nm, forcing EPA had to estimate high torque data with a conservative roll off in efficiency up to WOT The dashed black line in Figure 15 shows the extent of the original Honda data.

Thus, it is to be expected that EPA's engine map generated from its benchmarking data exhibits differences from the one generated from extrapolating Honda's published map. The differences outside of Honda's original data set (i.e., outside the dotted line box in Figure 15) are substantially due to estimates made by EPA to extend the map from Honda's published data.

Within the data set in Honda's image, EPA's map based on Honda published data was 1% to 2% BTE points less than the actual production engine at high torque levels (with a small island of nearly 4% at the extreme top of the map). Offsetting this, the EPA map based on Honda's published data was approximately 1% to 2% BTE point better than the EPA benchmark-based map at lower torques. Figure 15 also contains an image of the energy weighted operational cloud for this engine in a 2016 vintage mid-sized example vehicle driving over the combined regulatory cycles. This operational cloud reveals that most of the energy is used in the area centered about 1900 rpm and 70 Nm (indicated by the red hot-spot). At this point, the EPA BTE map based on test data is approximately 1.5% lower than the BTE map based on Honda's published image. The operational cloud shown is from an ALPHA simulation to illustrate about where the engine would run in a 2016 vintage standard-sized vehicle over the regulatory city/highway cycles. The cloud shows that the engine operation generally stays below 2500 rpm and a brake mean effective pressure (BMEP) of 14 bar.

The differences between the data sets are likely due to the calibration and hardware required for the specific application of the engine to the U.S. version of the 2016 Honda Civic. The Honda image the data could possibly be from a pre-production engine or an engine for a different market. The differences may also be attributable to minor changes between specific vehicle applications of the Honda L15B7 engine due to manufacturing variations between specific engines, test methods, test instrumentation, or a combination of these factors.

Comparison of CO_2 Predicted in ALPHA Using EPA Benchmarked and Honda Published Image Maps

As another comparison method, EPA's ALPHA model was used to predict differences in CO_2 emissions for these two engine maps over the combined EPA city/highway cycles used

for GHG compliance. These results are shown in Table 6 Part A as percent delta differences between the engine map generated from EPA benchmarked data and the one generated from Honda's published image of its map for the turbocharged engine.

The first row in Table 6 Part A contains a baseline estimate of 241.4 g/mile CO_2 from a 2016 vintage "typical" mid-sized car. The table shows a pair of ALPHA vehicle simulation results of an example 2016 mid-sized car weighing 3510 pounds; the top result uses the engine map from Honda published image, the bottom result of the pair uses the engine map from the EPA test data. The table also contains a second pair of ALPHA vehicle simulation results of an example 2025 mid-sized car weighing 3269 pounds with 10% lower aerodynamic resistance, 10% lower coefficient of rolling resistance, engine start-stop technology, and higher efficiency accessories [14]. Note that each of these engines has a slightly different displacement since when adapting an engine to a specific vehicle's technology package and roadload mix ALPHA resizes the engine displacement so that the vehicle's acceleration performance remains within 2% of the baseline vehicle as described in a previous EPA technical paper[15].

The vehicles use the set of A, B and C road-load coefficients shown in Table 6 Part B corresponding to the roadload for its model year. The A coefficient (lbs) represents a constant drag mostly from tire rolling resistance, B (lbs/mph) represents losses that increase with vehicle speed like bearing drag, and C (lbs/mph^2) represents losses that increase with the square of vehicle speed like aerodynamic drag.

The results using the map generated from the EPA test data from Honda's production engine have the higher CO_2 results of each pair over the regulatory drive cycles, corresponding to the lower BTE of the pair. The pair of simulations of the 2016 example vehicle shows a 1.1% increase in CO_2 over the regulatory cycles. The 2025 pair of simulations show a 0.9% increase in CO_2. The 1.1% to 0.9% increase in CO_2 is consistent with the roughly 1.5% decrease in BTE indicated at the hot-spot of weighted energy consumption in Figure 15, and confirms that the two maps are in good agreement when used over the regulatory cycles.

4. Comparison of the Honda Engine to Other Production Engines Using ALPHA

The next step in the engine benchmarking analysis for this paper uses EPA's ALPHA model to predict differences in CO_2 emissions over the combined EPA city/highway cycles used for GHG regulations. For comparison, a series of ALPHA simulations were run using the 2016 Honda engine alongside a 2010 Ford EcoBoost 1.6-liter engine and a 2015 Ford EcoBoost 2.7-liter engine. Both of these engines have been benchmarked by EPA previously, and complete engine maps are available for ALPHA simulations. The engine maps for each simulation were scaled to produce comparable vehicle performance consistent with the methods described in a previous EPA technical paper [15].

Table 7 shows how combined engine efficiency and combined CO_2 emissions change as the vehicle simulations change from 2016 to 2025 vintage (see Table 6 Part B to review how weight, road-load, transmission, start/stop, and engine accessories change between the two

vehicle vintages). The energy weighted engine efficiency between the 2016 and 2025 simulations increases approximately:

- 26.0% to 26.6% with EcoBoost 1.6-liter engine
- 27.0% to 27.5% with EcoBoost 2.7-liter engine
- 27.8% to 28.6% with benchmarked Honda 1.5-liter L15B7 engine

Table 7 shows that changing the engine from the EcoBoost 1.6-liter to the Honda 1.5-liter engine between the two simulations results in an impressive 6.8% reduction in CO_2 for the 2016 vintage vehicle and a 7.1%. reduction in CO_2 for the 2025 vintage vehicle.

5. Technology Comparison with Other Turbocharged Engines

The next section of the study compares technology in the Honda 1.5- liter engine to other engines on the market to better understand where the industry is heading. The efficiency of the Honda 1.5-liter L15B7 engine compares favorably to the two Ford EcoBoost engines, due in part to the advanced technologies incorporated in the Honda engine (see Table 1). In addition to Honda, a number of other manufacturers have recently announced or put into production turbocharged engines that have their own technology packages. To understanding how the new Honda boosted engine fits into the technology frontier of boosted engines being developed today, the technology content of these other engines was examined to determine the technology differences.

Engine Specifications:

To better understand the status of the industry's engine development, the technology content of a number of recently introduced or announced engines were compared. This list is not intended to all inclusive, but rather includes a sampling focused on boosted engines designed for the U.S. market and, with one exception, includes only engines with regular grade as the recommended fuel. Table 8 contains specifications of 10 different turbocharged engines. Table 9 contains a graphical summary of the technology content of each engine and its degree of implementation.

The list of engines in the two tables includes two older production engines from 2010 and 2015, four recent production engines from 2016 through 2018 (including the Honda 1.5-liter L15B7 engine presented in this paper), two emerging engines announced to enter production in the 2019 model year, and one future concept engine developed by Ricardo and EPA which was used within EPA's 2012 Regulatory Impact Analysis, 2016 Draft Technical Assessment, and 2016 Technical Support Document [14, 22, 24].

The list of engines is generally arranged from least to most technology content, starting with the Ford EcoBoost 1.6-liter introduced in 2010 and continuing through the EPA/Ricardo EGRB (exhaust gas recirculation with boosting) future concept engine. Detailed information regarding the EPA/Ricardo EGRB concept has been previously published [14, 16, 25]. Briefly, EGRB is a turbocharged GDI engine with an advanced boosting system, integrated exhaust manifold, cooled/external exhaust gas recirculation (EGR), discrete variable intake valve lift, and variable intake and exhaust valve timing.

Although this last engine in the table is a future concept engine that includes a number of advanced technologies, its estimated 37% peak efficiency has already been equaled or surpassed by a number of production engines, including the Honda 1.5-liter as shown by the two BTE maps in Figure 16. Although engine efficiency over the wider area of the engine map used during operation over regulatory cycles is more significant to determining CO_2 than peak engine efficiency, the increase in peak efficiency is a significant trend.

Engine Technology Content:

Using the data provided in Table 8, other manufacturer published information available at the time this paper was published [17–21], and engineering judgement, a comparative technology assessment was performed, with results shown in Table 9. Appendix C contains technical notes of how the color coding designations were determined for each technology in the table.

Table 9 provides a visual summary of each engine's "technology content along with some assessment of the degree of implementation of each technology. Some of the technologies in the table are either present or absent; these are reflected by red or green designation in Table 9. Other technologies have a range/gradient of implementation and effectiveness. For these technologies, yellow and light green designations were added to Table 9 to appropriately acknowledge the degree of implementation of the technology.

Table 9 provides a graphical summary of the technology content and level of implementation of technology for the chosen industry leading engines. The technology content of the engines generally increases as learning advances over time. There are a few key trends that can be observed from Table 8 and Table 9.

Trends:

Several engine parameters and technologies have been steadily advancing since 2010. These include compression ratio (CR), stroke/bore ratio, intake cam phase authority (as seen in Table 8). It also includes increased adoption of integrated exhaust manifolds, friction reduction, faster camshaft phasing control, advanced boosting technology, cooled EGR, and Miller cycle.

All of the technology included in the EPA/Ricardo EGRB engine and vehicle simulations from EPA's 2012 Regulatory Impact Analysis and other subsequent regulatory analyses [19–21] are gaining in use and maturity, are netting the efficiency benefits envisioned, and highlight the usefulness of engine combustion models and vehicle energy models in estimating the magnitude of potential future gains in efficiency.

In fact, as noted previously, the peak efficiency of the EPA/Ricardo EGRB engine has already been surpassed by the Honda engine. Although the Honda's performance over a wider area of operation is generally not quite as good as the Ricardo/EPA projection, as shown in Figure 16, the performance gap is closing significantly.

The steady improvement in peak and cycle efficiency advances with some of the newer engines shown in Table 8 appears to be due to the incorporation of multiple advanced

technologies, including continued reductions in parasitic losses (lower viscosity oil, for example), better boosting and boost control (see discussion in Appendix C), better charge mixing leading to improved knock mitigation and higher compression ratios, application of cooled EGR, and the emergence of fast wide-authority variable valve timing to enable Miller cycle modes of operation.

However, as seen in Table 9, no engine incorporates all potential improvements. There is significant untapped efficiency improvement potential still available for future vehicle use, both from the technology already implemented in some form in the current production engines listed, and from technology that has not been applied in combination with the other advanced technologies (e.g., cylinder deactivation, variable valve lift [VVL], variable compression ratio [VCR], and variations of dilute combustion/spark assisted gasoline compression ignition).

Finally, if Mazda follows its announced plans to introduce an engine with SPark Control Compression Ignition (SPCCI) with a peak efficiency of approximately 44%, the EPA/Ricardo target could be significantly exceeded.

6. Potential for Improving Efficiency

To build on the insights gained from comparing the Honda engine to other turbocharged engines on the market (or planned), this section explores the effects of adding some additional technologies onto the Honda engine. For the first example the comparison was accomplished with additional ALPHA simulations to estimate the potential efficiency improvements. Specifically, the CO_2 reduction benefits resulting from combining full continuous cylinder deactivation (deacFC) with EPA's fuel efficiency map from the benchmarking data of the Honda 1.5-liter L15B7 engine was modeled. The second example discusses the integration of advanced boosting technology, cooled EGR, and Miller cycle in future engines.

Example 1 Future Technology Combination: Honda 1.5-liter Turbocharged Engine with deacFC

As a case study of adding technology to the Honda 1.5-liter engine, the ALPHA model was used to perform full vehicle simulations of the same mid-sized exemplar vehicle defined in Table 6 Part B with a scaled turbocharged 1.5 liter L15B7 engine both with and without full continuous cylinder deactivation (deacFC). The energy weighted engine efficiency and CO_2 emissions over the combined cycle used for GHG certification and compliance in the U.S. (weighted city [FTP] and highway [HWFET] drive cycles) were compared.

DeacFC technology allows any of the cylinders of an engine to be deactivated, and the number of deactivated cylinders can be varied in a continuous fashion. For example, when an I4 engine with deacFC is running on two cylinders, any of the two cylinders can be firing and the firing cylinders can change to any two cylinders. In addition, the engine can be run on a non-integer number of cylinders (e.g., 2.5 cylinders) by varying the number and pattern of firing cylinders from one cycle to the next. DeacFC can also command complete cylinder

cut out during decelerations, cutting both fuel and air to the engine. This reduces aftertreatment cooling and vehicle deceleration.

Tula Technology developed an implementation of deacFC called Dynamic Skip Fire (DSF) and applied it to V8 and I4 engines. Tula explains how DSF reduces pumping and heat loss and avoids objectionable NVH in [26, 27].

For this illustration of applying deacFC to the Honda 1.5-liter engine, deacFC effectiveness and rules of application (fly zone) were based on EPA chassis dynamometer benchmarking of a Tula Technology deacFC-equipped 2011 Yukon Denali with a 6.2 liter L94 V8 engine [28], Tula and Delphi engine dynamometer testing of a deacFC- equipped 6.2 liter L94 V8 engine [29], and Tula and Delphi engine dynamometer testing of deacFC-equipped 1.8-liter turbo EA888 I4 engine [30].

EPA recognizes that deacFC effectiveness could scale with number of cylinders as a result of NVH constraints, so this analysis used for this paper assumes that engines with fewer cylinders have lower deacFC effectiveness [28]. NVH constraints in the application of deacFC to specific engines are discussed by Tula in [26].

Table 10 shows that application of deacFC to the Honda 1.5-liter engine, using EPA-estimated deacFC effectiveness [28], provides an estimated 0.8 percentage point increase in 2025 engine efficiency and a 2.6% drop in CO_2 emissions. Such a technology combination would be within about 5 grams of achieving the CO_2 reduction results of the targeted EPA/Ricardo EGRB24 engine, with a lower projected cost of implementation. Using deacFC effectiveness values from Tula publications [29, 30] would decrease CO_2 emissions by an additional 0.25% (not shown in the table). The engine maps for each simulation were scaled to produce comparable vehicle performance consistent with the methods described in a previous EPA technical paper [15].

Example 2 Future Technology Combination: Honda 1.5-liter Turbocharged Engine with Atkinson/Miller Cycle

Another case study example of a technology combination is integration of advanced boosting technology, cooled EGR, and Miller cycle within the Honda 1.5-liter L15B7 engine platform, a prominent focus of current and future development work in the industry and also the subject of further study by the EPA, due to its high potential to improve efficiency cost effectively.

Background of Atkinson Cycle ——Expanding combustion products to a lower pressure (potentially all the way to exhaust pressure), before opening the exhaust valve, allows for higher engine efficiency. An Atkinson- or Miller-cycle engine uses a high geometric compression ratio to achieve a high expansion ratio, and early intake valve closing (EIVC) or late intake valve closing (LIVC) is used to reduce effective compression ratio and improve knock tolerance. Drawbacks are less charge volume per unit exhaust stroke (i.e., a form of power density), and reduced charge motion and burn rate due to EIVC or LIVC.

Mazda initially began incorporating Atkinson cycle into their naturally aspirated SKYACTIV-G engine in 2012 and have since expanded this incorporation into boosted engines (Miller-cycle) like the 2016 2.5 L Mazda SKYACTIV-G and the announced 2.0L Mazda SKYACTIV-X. Other manufacturers are also adding Miller cycle to their boosted engines (e.g., 2018 2.0 L VW EA888, 2018 3.0 LVW/Audi EA839, and 2018 2.1 L Nissan MR20 DDT).

Quantification of Degree of Atkinson -—There are numerous ways to quantify the degree to which an engine uses Atkinson or Miller cycle at a given operating point, including:

1. Ratio of expansion and compression strokes (m/m)
2. Ratio of expansion and compression volume ratios (m^3/m^3)
3. Over-expanded Otto cycle fuel conversion efficiency (%)
4. Over-expanded Otto cycle with pumping loop (%)

Each method has certain advantages and limitations but method (2) was used to compare the engines in this study.

The naturally aspirated 2012 Mazda SKYACTIV-G 2.0 L, which has a geometric compression and expansion volume ratio of 13.0:1, uses a high degree of Atkinson cycle. As shown in Figure 17, the Mazda 2.0 L achieves a maximum re/rc (ratio of expansion and compression volume ratios) of over 1.8.

In comparison as shown in Figure 18, the 2016 Honda 1.5-liter L15B7 engine (and approximately half of the other boosted engines reviewed for this paper) does not apply an appreciable degree of Miller cycle. The Honda engine applies a maximum r_e/r_c of 1.05. Other boosted engines are known to be beginning to apply more Miller cycle operation, including the 2016 Mazda 2.5 L, 2018 VW2.0 L, 2018 VW/Audi 3.0 L, and 2019 Mazda 2.0 L, however, the Atkinson ratio estimates were not available to the EPA in time for publication in this paper.

The Miller cycle is expected to be applied to increasing numbers of boosted engines as development engineers use boosting to overcome reduced power density (less charge per unit exhaust stroke) and implement various methods of increasing charge motion (e.g., increased tumble).

Summary/Conclusions

The benchmarking test method of mapping an engine by tethering a vehicle to an engine in an engine dynamometer cell has been expanded to include a more robust high load test procedure that captures the transient nature of the operation of the engine in the high load region where enrichment occurs.

The new test procedures developed, along with traditional steady-state test procedures and low-speed test procedures incorporating a transmission, enabled the testing of the engine

over its full operating range, including idle, low to high load at stoichiometric and high load with commanded fuel enrichment.

The BTE map for the Honda L15B7 engine developed from the benchmark testing shows the highest efficiency of any publicly available map for a production turbocharged engine. The map developed from benchmarking is similar to a map previously published by Honda for a development version of this same 1.5-liter engine.

A review of other current production turbocharged engines shows continuous steady progress in technology adoption and efficiency improvement that is approaching the efficiency of the EPA projection of a future advanced technology turbocharged engine based on the modeling of the EPA/Ricardo EGRB24 engine. Many of the technologies included in this future concept engine are already incorporated in recent production engines and additional technologies not anticipated in EPA's 2012 Regulatory Impact Analysis have appeared on engines in the marketplace.

Significant untapped efficiency improvement potential is still "on the table," both from the technology already implemented in some form in the current production engines listed, and from technology that has not even been applied in combination with the other advanced technologies (e.g., fixed cylinder deactivation, full continuous cylinder deactivation, VVL, Miller cycle, VCR, and variations of gasoline compression ignition).

Acknowledgments

The authors would like to thank Kevin Newman, Karla Butters, Brian Olson, Raymond Kondel, Mike Murphy, and Greg Davis in the National Center of Advanced Technology at the National Vehicle and Fuel Emissions Laboratory for their assistance and contribution to perform necessary engine testing and ALPHA modeling.

Appendix A

Benchmarking Plots for the Honda 1.5-liter L15B7 Engine

Note: Several of these figures include both "Initial" and "Final" windows of operation to show how measured parameters change in high load region. The initial window is just after torque value is reached and the final value is after several seconds of operation when engine controls stabilize.

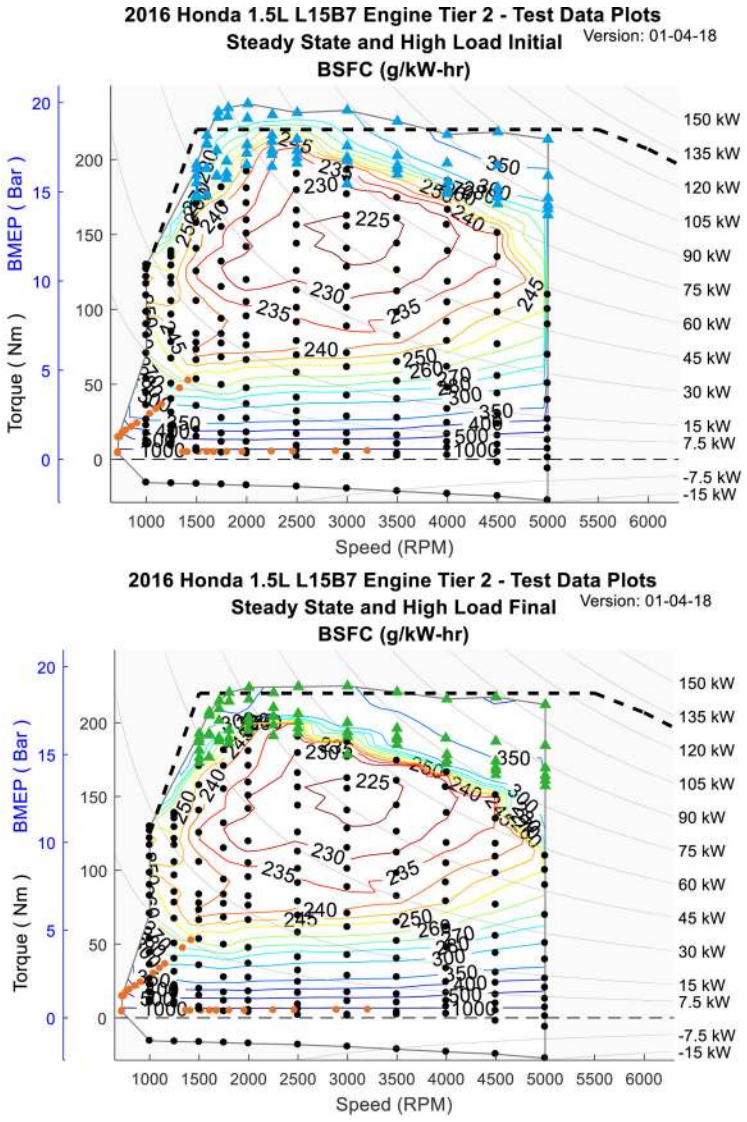

Figure A1.

Steady-State and High Load Initial and Final **BSFC Maps** for the 2016 Honda 1.5-liter L15B7 Engine

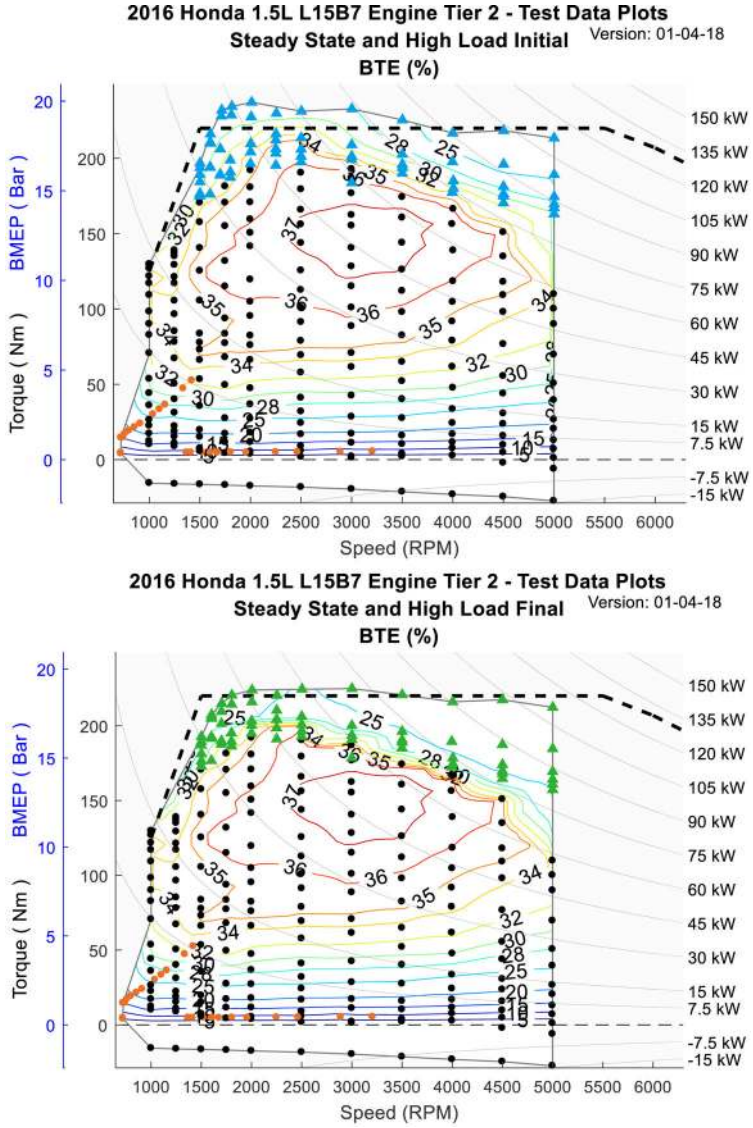

Figure A2.

Steady-State and High Load Initial and Final **BTE Maps** for the 2016 Honda 1.5-liter L15B7 Engine

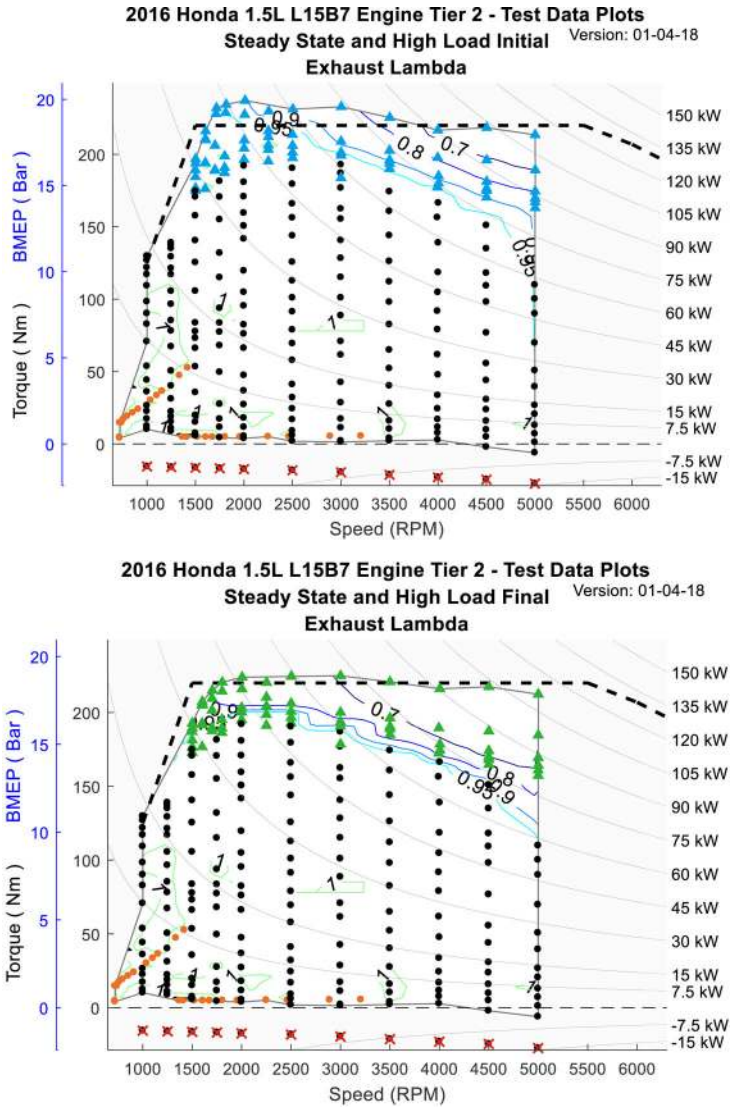

Figure A3.

Steady-State and High Load Initial and Final **Exhaust Lambda Maps** for the 2016 Honda 1.5-liter L15B7 Engine (Note: The air-fuel ratio analyzer contains a wideband oxygen sensor which is operated per factory suggested settings.)

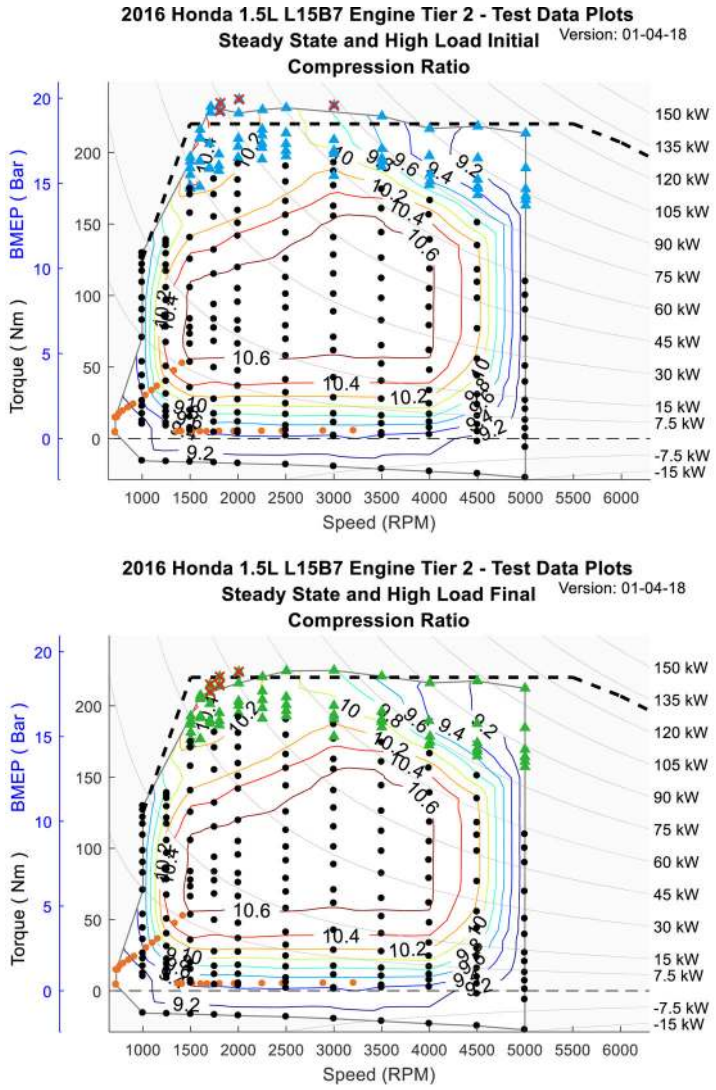

Figure A4.

Steady-State and High Load Initial and Final **Compression Ratio Maps** for the 2016 Honda 1.5-liter L15B7 Engine (Note: event locations are determined at 1mm valve lift)

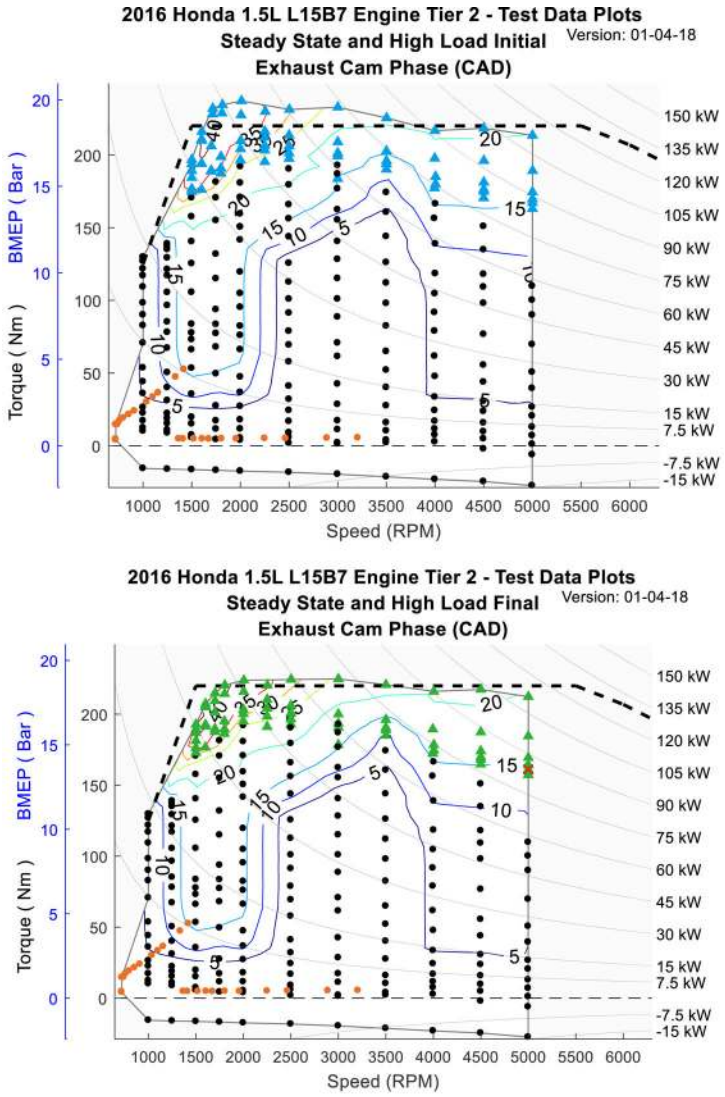

Figure A5.

Steady-State and High Load Initial and Final **Exhaust Cam Phase Maps** for the 2016 Honda 1.5-liter L15B7 Engine (Note: phase is measured relative to the VVT actuator parked position)

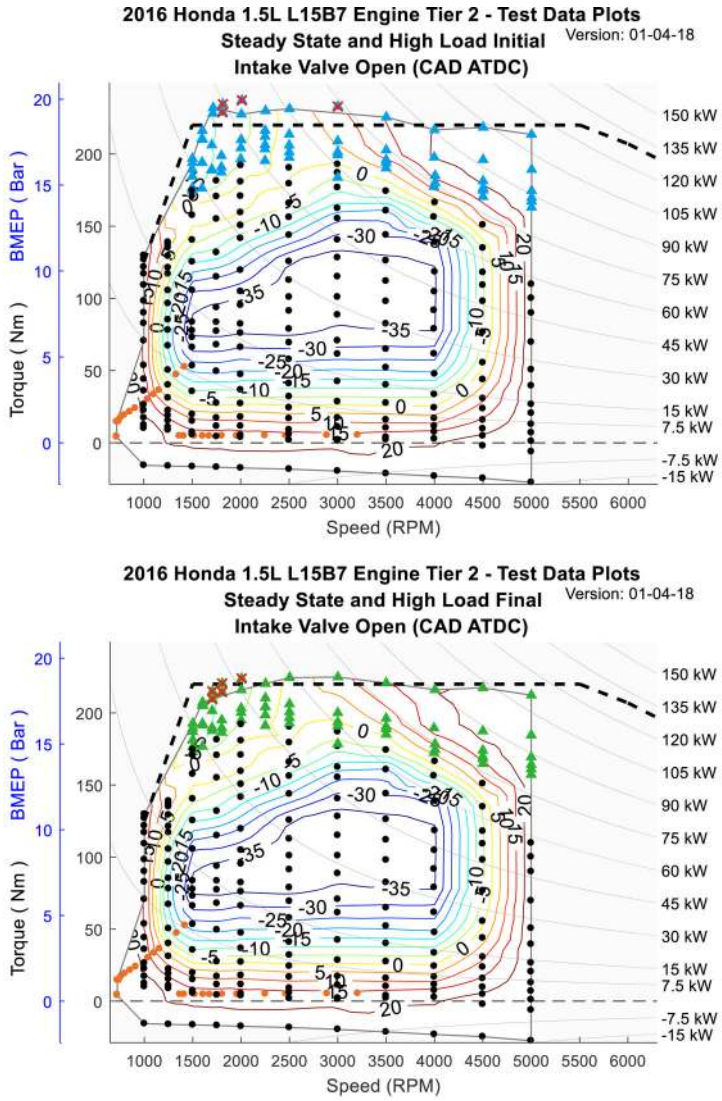

Figure A6.

Steady-State and High Load Initial and Final **Intake Cam Phase Maps** for the 2016 Honda 1.5-liter L15B7 Engine (Note: phase is measured relative to the VVT actuator parked position)

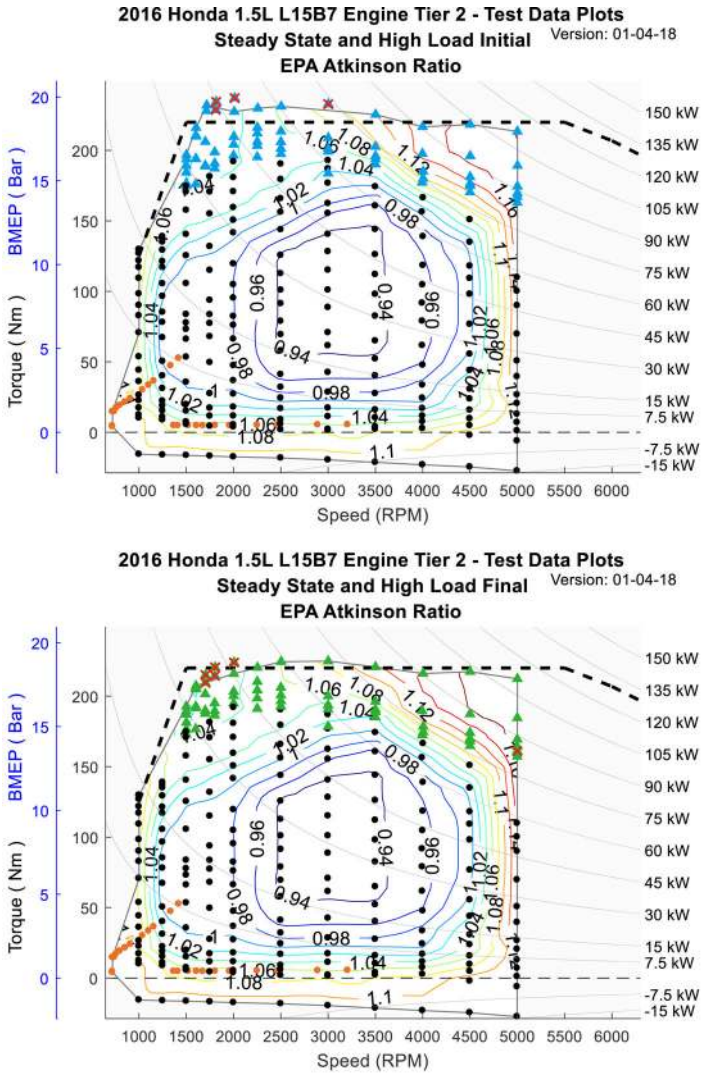

Figure A7.

Steady-State and High Load Initial and Final **Atkinson Ratio Maps** for the 2016 Honda 1.5-liter L15B7 Engine (For this study, the Atkinson Ratio is the ratio of effective expansion stroke length to effective compression stroke length where the extremity of each stroke is determined by the location corresponding to 1mm of valve lift.)

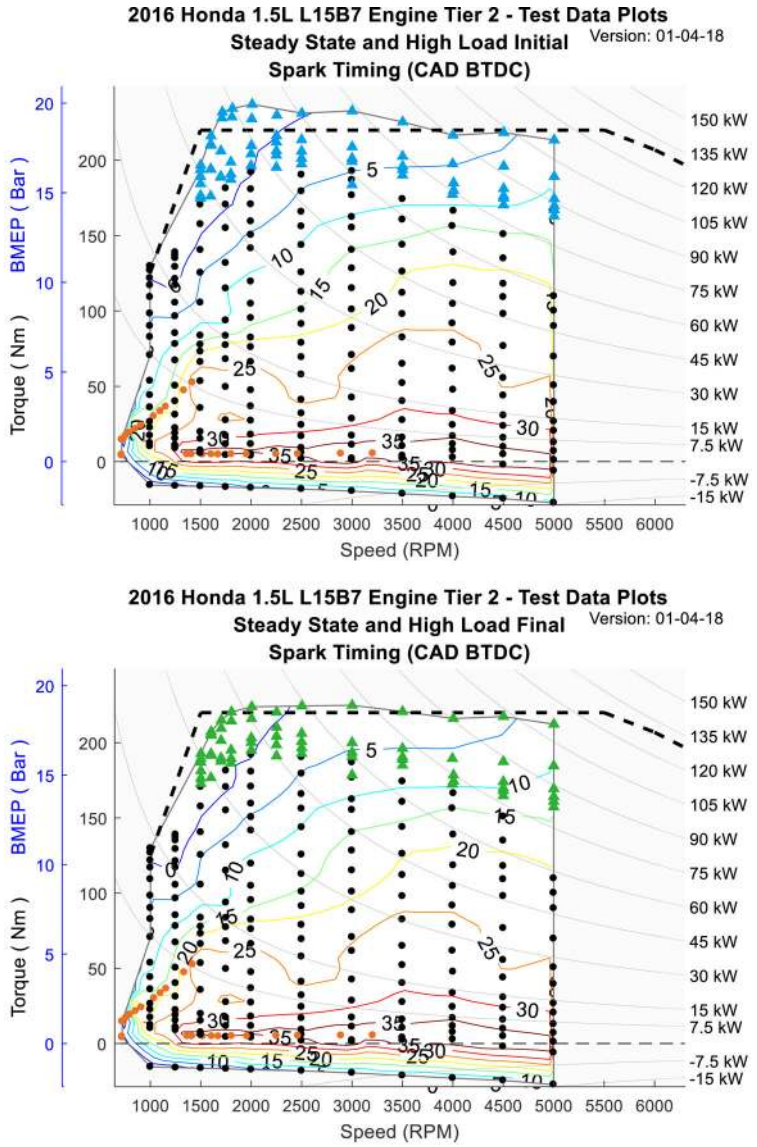

Figure A8.

Steady-State and High Load Initial and Final **Spark Timing Maps** for the 2016 Honda 1.5-liter L15B7 Engine

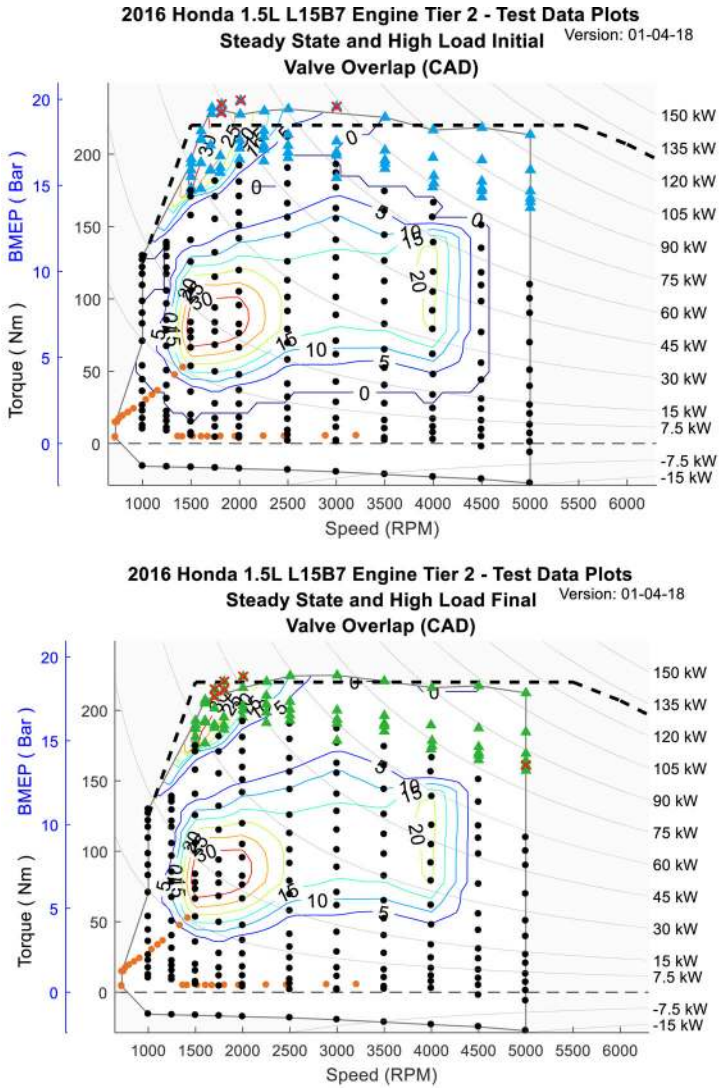

Figure A9.

Steady-State and High Load Initial and Final **Valve Overlap Maps** for the 2016 Honda 1.5-liter L15B7 Engine (Note: valve opening and closing events are defined by 1 mm valve lift)

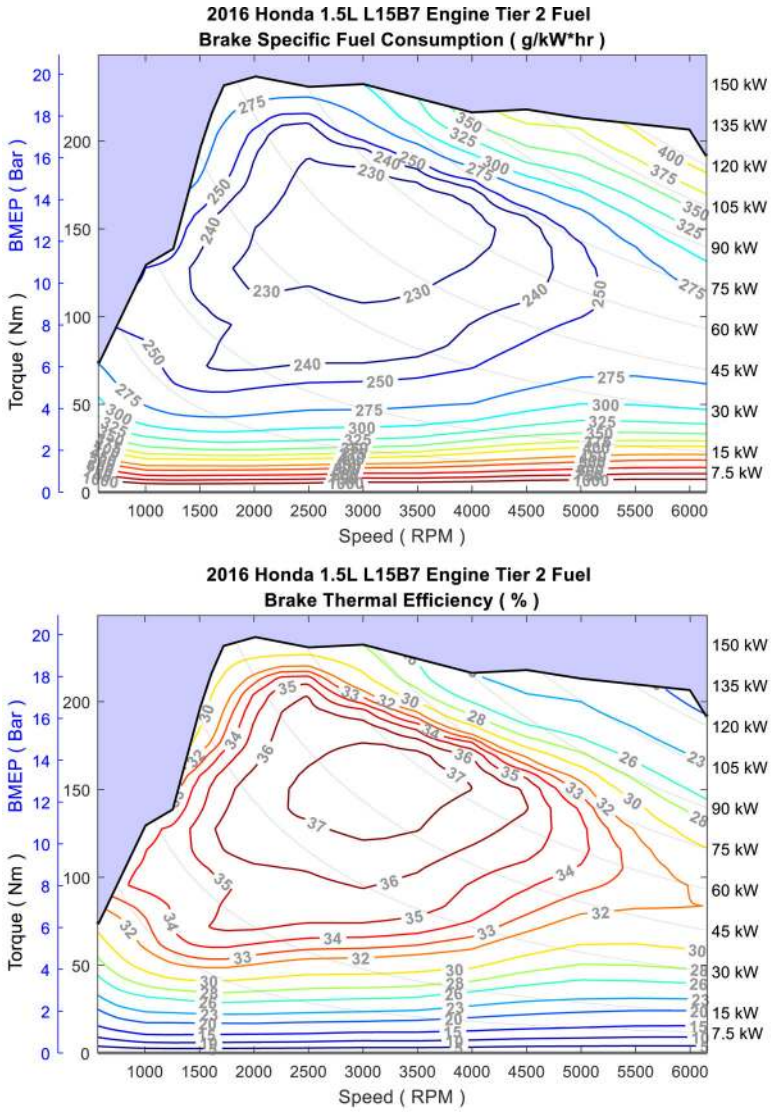

Figure A10.
Complete_ALPHA **BSFC and BTE Maps** for the 2016 Honda 1.5-liter L15B7 Engine - Tier 2 fuel

Appendix B

Honda 1.5-liter L15B7 Engine - Effect on BTE using Tier 2 versus Tier 3 Fuel

The Honda 1.5-liter L15B7 engine was benchmarked by EPA with two different fuels - EPA Tier 2 and Tier 3 Certification fuels. See Table 4 in the body of the paper for the fuel specifications. The steady-state mapping was repeated for each fuel. Prior to testing, the engine and ECU were taken through a preparatory run with the specific fuel for the ECU to actively adjust to the change in octane and alcohol content. This procedure consisted of running the engine at medium to high loads for an extended period.

The steady-state mapping results do show some brake thermal efficiency differences between the two fuels. Figure B1 is an example data set at 1500 rpm showing the effect of the two different fuels on BTE. The data points shown in Figure B1 are load points that are at stoichiometric A/F ratio. Higher load points that include commanded fuel enrichment are not shown.

Other BTE data from the benchmark testing on this engine using the two fuels show the same type of BTE behavior at different engine rpm settings. Figure B2 shows the effect on BTE at 2000 rpm.

It is important to note that the drop in BTE with Tier 3 fuel does not actually correspond to a similar increase in CO_2 emissions because Tier 3 fuel has a lower carbon content than Tier 2 fuel. Other EPA testing on this subject has shown that these effects typically offset over the U.S. regulatory drive cycles, and in fact, using Tier 3 fuel results in a small-but-measurable overall reduction in CO_2 both on a fleet-wide basis and for the Honda L15B7, as installed in the 2016 Honda Civic. Data on EPA's work on CO_2 emissions impacts, including the tests for statistical significance of the data, were presented in the following reference [14].

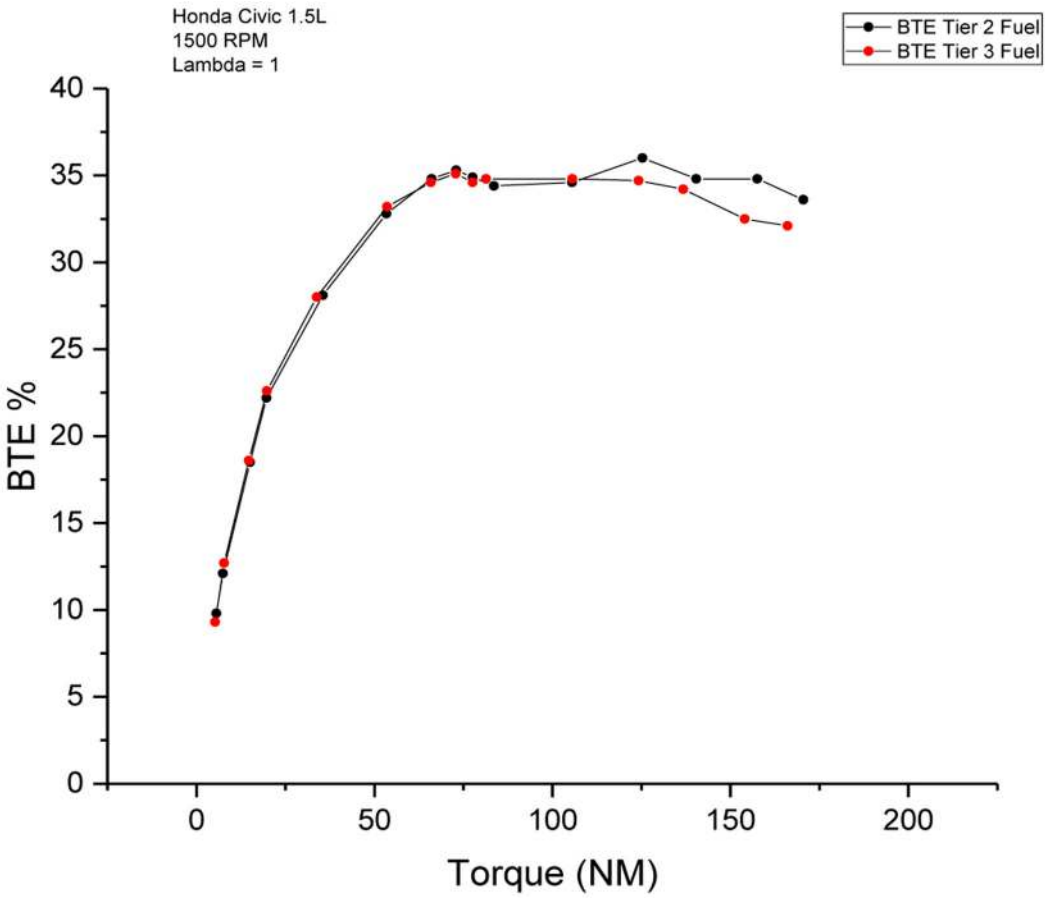

Figure B1.
Effect of different fuels on BTE at 1500 rpm (all points are in stoichiometric operation)

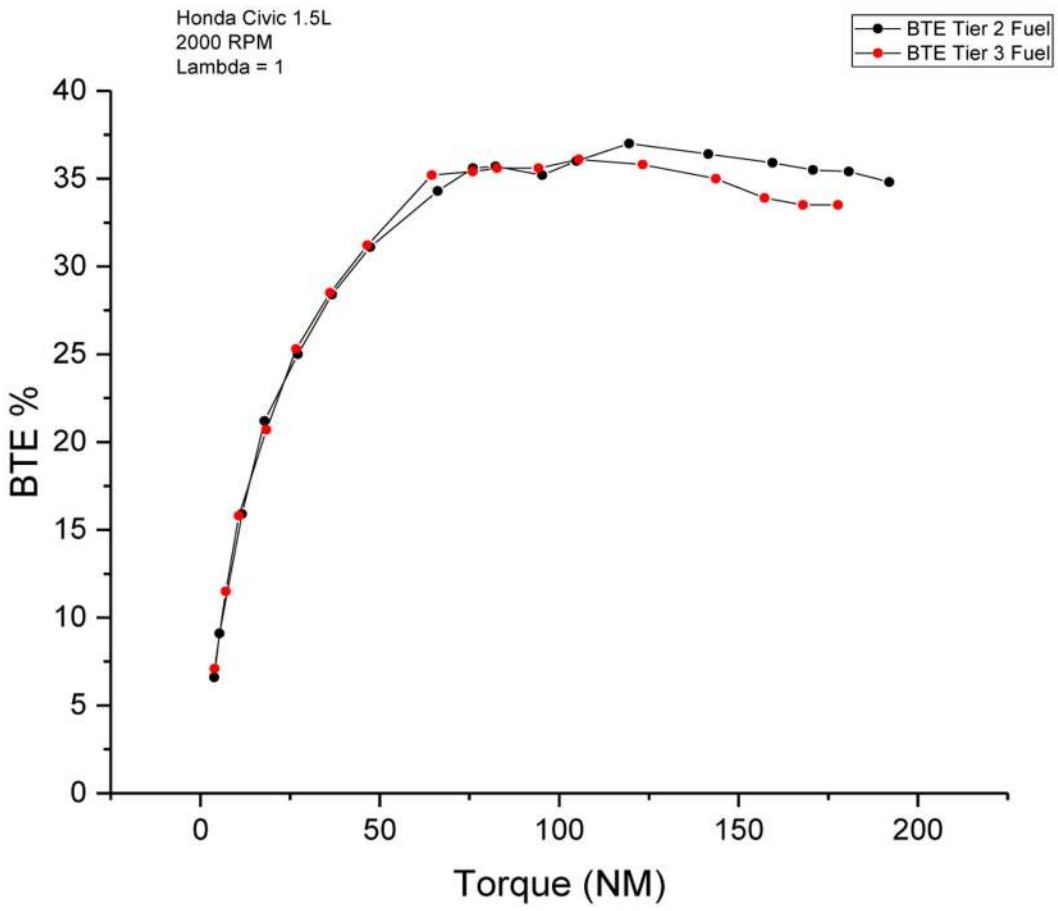

Figure B2.
Effect of different fuels on BTE at 2000 rpm (all points are in stoichiometric operation)

Appendix C

Characterization of "Degree of Implementation" of the Technologies in Selected Turbo Charged Engines

This Appendix contains the detailed analysis notes of the characterization criteria used to assign the colors to the cells in "Table 9: *Technology content and degree of implementation*" in the body of the paper.

Table 9 represents a graphical color-coded view of a comparative assessment of the 14 different technologies in the 10 different engines. The color coding in that table is based upon engine specification information in "Table 8: *Summary of turbocharged engine specifications*" also in the body of the paper, manufacturer published information available at the time the paper was published [17–21], and engineering judgement.

Engine Technologies That Are Either "Present or Absent"

Ten of the technologies, represented by the columns with red text titles in the Table 9, are either present in the specific engine (the row), or they are absent. Within these columns, the color of the cell indicates the presence of the technology (dark green cell) or absence of the technology (red cell). A grey cell was used if the existence of the technology was unknown.

These technologies listed in Table 9 which are either present or absent are:

1. Variable Valve Timing (VVT)
2. Integrated Exhaust Manifold
3. cooled EGR
4. Variable Valve Lift (VVL)
5. Miller Cycle
6. VNT / VGT Turbo
7. Partial Discrete Cylinder Deactivation (deacPD)
8. Full Continuous Cylinder Deactivation (deacFC)
9. Variable Compression Ratio (VCR)
10. Gasoline Compression Ignition

Engine Technologies That Have A "Degree of Implementation"

The remaining four technologies in Table 9, represented by the columns with white text titles, can have a range or gradient of implementation and effectiveness. These technologies are:

1. High Geometry CR
2. Friction Reduction
3. Higher Stroke/Bore ratio
4. Boosting Technology

For these technologies, a yellow or light green coloring was used in addition to the red and dark green coloring to appropriately acknowledge a "degree of implementation" for the technology. In this case, the red coloring indicates the absence of the technology, yellow indicates an early implementation, and light and dark green indicates implementations which are nearing maturity. This assessment is based upon information in Table 8, manufacturer published information, and engineering judgement.

Characterization Notes:

1. **High Geometric Compression Ratio** -- The assessment of the geometric compression ratio is based on the "compression ratio" data in Table 8. Engines with a higher compression ratio tend to have a higher efficiency. Engines with

geometric compression ratios of 10.0 were designated by yellow, those with compression ratios near 10.3 were designated by light green, and those with compression ratios of 11.0 or larger were designated by a dark green.

2. **Friction Reduction** -- The assessment of friction reduction is based on the vintage of the engine and based on oil viscosity as a surrogate indicator in Table 8. The Ford EcoBoost 1.6L engine, the only engine designated by yellow, was introduced in 2010 and thus is assumed to have less friction reduction than 2015 and later engines. Friction reduction technologies include use of lower viscosity and lower friction lubricants, low-tension piston rings, roller cam followers, roller bearings for balance shaft systems, improved engine thermal management, improved production tolerances, piston surface treatments, cylinder wall treatments, improved material coatings such as diamond-like-carbon coatings, and other improvements in the design of engine components and subsystems that improve friction or reduce parasitic losses from the lubricating system.

   The three engines with 0w oil – the Honda L15B7, VW EA888, and the VW EA211 – were designated by dark green. The remaining engines were designated by light green. The viscosity of the oil used in the VW EA839, Nissan MR20, and Mazda Skyactiv-X engines is unknown, so these engines were tentatively assigned designated by light green, although the friction reduction may be more substantial.

3. **Higher Stroke/Bore Ratio** - The assessment of stroke-to-bore ratio is based on the stroke/bore data in Table 8. A higher stroke-to-bore ratio promotes better tumble, better mixing, and helps mitigate against knock. Stroke/bore ratios between 0.96 and 1.03 were designated by red, stroke/bore ratios between 1.05 and 1.09 were designated by yellow, stroke/bore ratios between 1.12 and 1.15 were designated by light green, and stroke/bore ratios over 1.2 were designated by dark green.

4. **Boosting Technology** -- The assessment of boosting technology is based on the relative efficiency of the boosting system. Not all turbocharger systems are created equal, and some additional gradation is appropriate when assessing future potential still available.

   For example, the Ford EcoBoost 1.6-liter engine uses boost pressure actuated wastegate that can’t operate until boost pressure is available at approximately mid-load. Thus, at lower loads experience over the regulatory cycles, all the exhaust flows through the turbo turbine, resulting in added back pressure and loss in engine efficiency. Later turbo implementations improved on this, and thus the Ford EcoBoost 1.6L is designated by a yellow cell.

   The Ford 2.7-liter engine uses a vacuum-actuated wastegate which can be opened in the non-boosted load range. This reduces pumping losses compared to the previous 1.6L EcoBoost engine. The 2.7L also has an integrated exhaust manifold which lowers the turbine inlet temperature, allowing less enrichment at high load. Thus, this engine is designated by a light green cell.

The Honda 1.5-liter engine uses an electrically actuated wastegate, which allows the wastegate to be used at low to mid load, eliminating the back pressure and efficiency loss of the pressure actuated system used in the Ford 1.6-liter engine, and thus this engine is designated by a light green cell.

The Mazda Skyactiv-G 2.5-liter engine adds a unique flapper valve in the exhaust to provide a way to optimize both low speed torque and high speed power/torque, similar to what a variable geometry turbo provides, resulting in higher overall performance and efficiency, and thus is designated by a dark green cell.

Likewise, the VW EA211 has a variable nozzle turbine (VNT), so it is designated by dark green.

The Mazda Skyactiv-X is very high efficiency spark control compression ignition (SPCCI) engine which uses a mechanically-driven supercharger to enable. Although only limited information on this engine is available, it is likely that the supercharger is used in part to drive external EGR and may also be used to increase peak BMEP. The choice of mechanically-driven supercharger, as opposed to turbocharging, may be due to insufficient exhaust energy to effectively drive the exhaust turbine. It is possible that future generations of SPCCI could improve the boosting system to further increase efficiency. While additional improvements from further boosting refinements are still possible, we still chose to designate the cell for this engine with dark green.

The EPA/Ricardo EGRB24 engine incorporates a VNT, and is also designated by dark green.

The specifics of the boost systems of the VW EA888 and the VW EA839 indicate that they are twin-scroll turbos with pneumatically-actuated wastegate and thus designated by a light green cell.

Finally, the boost systems for Nissan MR20 is unknown and thus designated by a grey cell.

5. **Variable Valve Lift (VVL)** -- The assessment of variable valve lift is based on the existence of a VVL system on the engine. Engines without variable lift are designated by red cells. Four engines - the VW EA888–3B, VW EA211 EVO, VW/Audi EA839, and EPA/Ricardo EGRB24 - all have VVL and therefore are designated by dark green.

6. **VNT / VGT Turbo** -- The assessment of variable nozzle turbines (VNTs) or variable-geometry turbochargers (VGTs) is based primarily on the existence of the technology. The only engines with a continuously variable VNT / VGT are the VW EA211 and the EPA/Ricardo EGRB24, which are designated by dark green.

Definitions/Abbreviations

A/F	Air Fuel ratio

AKI	Anti-Knock Index
ALPHA	Advanced Light-duty Powertrain and Hybrid Analysis Tool
BCM	Body Control Module
BMEP	Brake Mean Effective Pressure
BSFC	Brake Specific Fuel Consumption
BTE	Brake Thermal Efficiency
b	Regression Offset
CAD	Crank Angle Domain
CAN	Control Area Network
CAS	Combustion Analysis System
CO_2	Carbon Dioxide
COV	Coefficient of Variation
CFR	Code of Federal Regulations
CVT	Continuously Variable Transmission
deacFC	Full Continuous Cylinder Deactivation
deacPD	Partial Discrete Cylinder Deactivation
dur_{inj}	Injector-open during (time)
ECU	Engine Control Unit
EGR	Exhaust Gas Recirculation
EGRB	Exhaust Gas Recirculation with Boosting
EIVC	Early Intake Valve Closing
EPA	U.S. Environmental Protection Agency
FE	Fuel Economy
FTP	U.S. Light-duty Federal Test Procedure or City Cycle
FEAD	Front End Accessory Drive GHG Greenhouse Gas
GHG	Greenhouse Gas
I/O	Input/Output
I4	Inline 4-cylinder Engine
HWFET	U.S. Light-duty Highway Fuel Economy Test or Highway Cycle

LD	Light Duty
LFE	Laminar Flow Element
LIVC	Late Intake Valve Closing
m	Regression Slope
NCAT	National Center for Advanced Technologies
NVFEL	National Vehicle and Fuel Emissions Laboratory
NVH	Noise, vibration, harshness
OBD	Onboard Diagnostics
PFI	Port Fuel Injection
$\mathbf{P_{rail}}$	High-pressure Fuel Rail Pressure
$\mathbf{q_{fuel}}$	Injected fuel quantity
RL	Road Load
RPECS	Rapid Prototyping Electronic Control System
SPCCI	SPark Control Compression Ignition
SwRI	Southwest Research Institute
US06	U.S. Supplemental Federal Test Procedure High-speed/Aggressive Driving Cycle
V8	Vee-configured 8-cylinder Engine
VCR	Variable Compression Ratio
VGT	Variable-Geometry Turbocharger
VNT	Variable Nozzle Turbine
VVL	Variable Valve Lift
VVT	Variable Valve Timing
WOT	Wide open throttle

References

1. Lee B, Lee S, Cherry J, Neam A, et al., “Development of Advanced Light-Duty Powertrain and Hybrid Analysis Tool,” SAE Technical Paper 2013-01-0808, 2013, doi:10.4271/2013-01-0808.
2. Kargul J, Moskalik A, Barba D, Newman K, et al., “Estimating GHG Reduction from Combinations of Current Best-Available and Future Powertrain and Vehicle Technologies for a Midsized Car Using EPA’s ALPHA Model,” SAE Technical Paper 2016-01-0910, 2016,doi: 10.4271/2016-01-0910.

3. Niizato T, Yasui Y, Urata Y Wada Y, Jono M, Nakano K, and Taguchi M "Honda's New Turbo-GDI Engine Series for Global Application." 37th International Vienna Motor Symposium, 2016.
4. Wada Y, Nakano K, Mochizuki K, and Hata R, "Development of a New 1.5L I4 Turbocharged Gasoline Direct Injection Engine," SAE Technical Paper 2016-01-1020, 2016, doi: 10:4271/2016-01-1020.
5. U.S Code of Federal Regulations, Title 40, Part 1065, §1065.130, 1 1, 2018.
6. Stuhldreher M, Schenk C, Brakora J, Hawkins D, et al., "Downsized Boosted Engine Benchmarking and Results,"SAE Technical Paper 2015-01-1266, 2015, doi:10.4271/2015-01-1266.
7. Ellies B, Schenk C, and Dekraker P, "Benchmarking and Hardware-in-the-Loop Operation of a 2014 MAZDA SkyActiv 2.0 L 13:1 Compression Ratio Engine," SAE Technical Paper 2016-01-1007, 2016, doi:10.4271/2016-01-1007.
8. Stuhldreher M, "Fuel Efficiency Mapping of a 2014 6- Cylinder GM EcoTec 4.3 L Engine with Cylinder Deactivation," SAE Technical Paper 2016-01-0662, 2016, doi:10.4271/2016-01-0662.
9. U.S. EPA. "2013 Chevrolet Malibu 2.5 L Engine Mapping Test Package." Docket number EPA-HQ-OAR-2015-0827- 0532. Also available at https://www.epa.gov/sites/production/files/2016-10/2013-chevrolet-malibu-2.5l-engine-mapping-test-package-06-20-16.zip. Last accessed onJanuary 3, 2018.
10. U.S. EPA. "2014 Mazda 2.0 L Skyactiv 13–1 Tier 2 Fuel Engine Mapping Core Test Package." Docket number Nissan HQ-OAR-2015-0827-0533. Also available at https://www.epa.gov/sites/production/files/2016-10/2014-mazda-2.0l-skyactiv-13-1-tier2-fuel-engine-mapping-core-test-package-06-28-16.zip (last accessedJanuary 3, 2018).
11. U.S. EPA. "2015 Ford F150 2.7 L Tier 2 Fuel - Engine Mapping Core Test Package." Docket number EPA-HQ-OAR-2015-0827-0534. Also available at https://www.epa.gov/sites/production/files/2016-10/2015-ford-f150-2.7l-tier2-fuel-engine-mapping-core-test-package-06-21-16.zip (last accessedJanuary 3, 2018).
12. Furukawa T, Okada N, Honda I, and Akiba A "Automobile Efficiency Improvements Using Electrochemical Capacitor Energy Storage." Proceedings of Electrical Vehicle Symposium 27, 2013 DOI: 10.1109/EVS.2013.6914977.
13. Dekraker P, " Constructing Engine Maps for Full Vehicle Simulation Modeling," SAE Technical Paper 2018-01-1412, 2018, doi:10.4271/2018-01-1412.
14. U.S. EPA. Proposed Determination on the Appropriateness of the Model Year 2022–2025 Light-Duty Vehicle Greenhouse Gas Emissions Standards under the Midterm Evaluation: Technical Support Document. §2.3.4.1.9.1 -Effectiveness Data Used and Basis for Assumptions. Document Number EPA-420-R-16–021, 11 2016.
15. Dekraker P, Kargul J, Moskalik A, Newman K et al., "Fleet-Level Modeling of Real World Factors Influencing Greenhouse Gas Emission Simulation in ALPHA," SAE Int. J. Fuels Lubr 10(1):2017, doi:10.4271/2017-01-0899.
16. Ricardo, "Computer Simulation of Light-Duty Vehicle Technologies for Greenhouse Gas Emission Reduction in the 2020–2025 Timeframe," EPA-420-R-11-020, 2011.
17. Hirose I Mazda 2.5 L SKYACTIV-G Engine with New Boosting Technology. 37th International Vienna Motor Symposium, 2016.
18. Wurms R, Budack R, Grigo M, Mendl G, Heiduk T, and Knisch S The New Audi 2.0 L Engine with Innovative Rightsizing – a Further Milestone in the TFSI Technology. 36th Vienna Motor Symposium, 2015.
19. Eichler F, Demmelbauer-Ebner W, Theobald J, Stiebels B, Hoffmeyer H, and Kreft M The New EA211 TSI® evo from Volkswagen. 37th Vienna Motor Symposium, 2016.
20. Königstedt J, Bonn G, Brinkmann C, Fröhlich G, Heiduk T, and Jablonski J The New 3.0l V6 TFSI Engine from Audi. 37th Vienna Motor Symposium, 2016.
21. Kiga S, Moteki K, and Kojima S The World's First Production Variable Compression Ratio Engine - The New Nissan VC-T (Variable Compression-Turbo) Engine. 38th Vienna Motor Symposium, 2017.
22. U.S. EPA. "Regulatory Impact Analysis: Final Rulemaking for 2017–2025 Light-Duty Vehicle Greenhouse Gas Emission Standards and Corporate Average Fuel Economy Standards." Document Number EPA-420-R-12-016, 8 2012.

23. U.S. EPA. Proposed Determination on the Appropriateness of the Model Year 2022–2025 Light-Duty Vehicle Greenhouse Gas Emissions Standards under the Midterm Evaluation: Technical Support Document. Document Number EPA-420-R-16-021, 11 2016.
24. U.S. Environmental Protection Agency. “Draft Technical Assessment Report: Midterm Evaluation of Light-Duty Vehicle Greenhouse Gas Emission Standards and Corporate Average Fuel Economy Standards for Model Years 2022 2025”. Document Number EPA-420-D-16-900, 7 2016.
25. Cruff L, Kaiser M, Krause S, Harris R et al., “EBDI® - Application of a Fully Flexible High BMEP Downsized Spark Ignited Engine,” SAE Technical Paper 2010-01-0587, 2010, doi: 10.4271/2010-01-0587.
26. Serrano J, Routledge G, Lo N, Shost M, Srinivasan V, Ghosh B, “Methods of Evaluating and Mitigating NVH when Operating an Engine in Dynamic Skip Fire,” SAE Technical Paper 2014-01-1675, 2014.
27. Eisazadeh-Far K, Younkins M, “Fuel Economy Gains Through Dynamic-Skip-Fire in Spark Ignition Engines,” SAE Technical Paper 2016-01-0672, 2016.
28. Bohac S, “Benchmarking and Characterization of Two Cylinder Deactivation Systems - Full Continuous and Partial Discrete,” SAE Oral-Only Presentation, SAE World Congress, 2018.
29. Younkins M, Tripathi A, Serrano J, Fuerst J, Schiffgens HJ, Kirwan J, Fedor W, “Dynamic Skip Fire: The Ultimate Cylinder Deactivation Strategy,” 38th International Vienna Motor Symposium, 2017.
30. Fuschetto J, Eisazadeh-Far K, Younkins M, Carlson S, Confer K, Fedor W, Kirwan J, “Dynamic Skip Fire in Four-Cylinder Spark Ignition Engines: Fuel Economy Gains and Pollutant Emissions Reductions,” SAE Oral-Only Presentation, SAE World Congress, 2017.

Test Phase 1: Low-Mid Loading

To collect the black dot data points in Figure 5, the engine is configured without its CVT, tested in steady-state operation at low to mid loads where the air-to-fuel (A/F) ratio remains stoichiometric at speeds from 1000 to 5000 rpm, and using the steady- state data collection and steady-state processing with the iTest system.

Test Phase 2: High Loading

To collect the blue triangle and green square data points in Figure 5, the engine is configured without its CVT, tested in transient operation at high loads where the air-to-fuel (A/F) ratio will transition to enriched to protect the engine at speeds of1000 to 5000 rpm, and using the transient data collection procedure and the initial-final interval post-processing.

Test Phase 3: Idle-Low Loading

The engine is configured with its CVT, tested in steady-state operation at low torque loads where the air-to-fuel (A/F) ratio remains stoichiometric at speeds from idle to approximately 3000 rpm, using the steady-state data collection and steady-state processing within the iTest data acquisition system for the red *x* and orange + data points in Figure 5.

Injector Fuel Flow Correlation

The relationship between fuel rail pressure, injection duration and injected fuel quantity for a single injection event follows from the classic orifice equation and is shown in Equation 1.

$$q_{fuel} = m \cdot \left(\sqrt{P_{rail}} \cdot dur_{inj}\right) + \mathrm{b} \quad (1)$$

Where: q_{fuel} = injected fuel quantity (mg)

p_{rail} = High pressure fuel rail pressure (MPa)

dur_{inj} = Injector open duration (ms)

The calibration constants m (slope) and b (offset) can be determined via linear regression. Figure 8 below shows an example of the relationship from test data obtained testing a Honda L15B7 1.5l turbocharged engine.

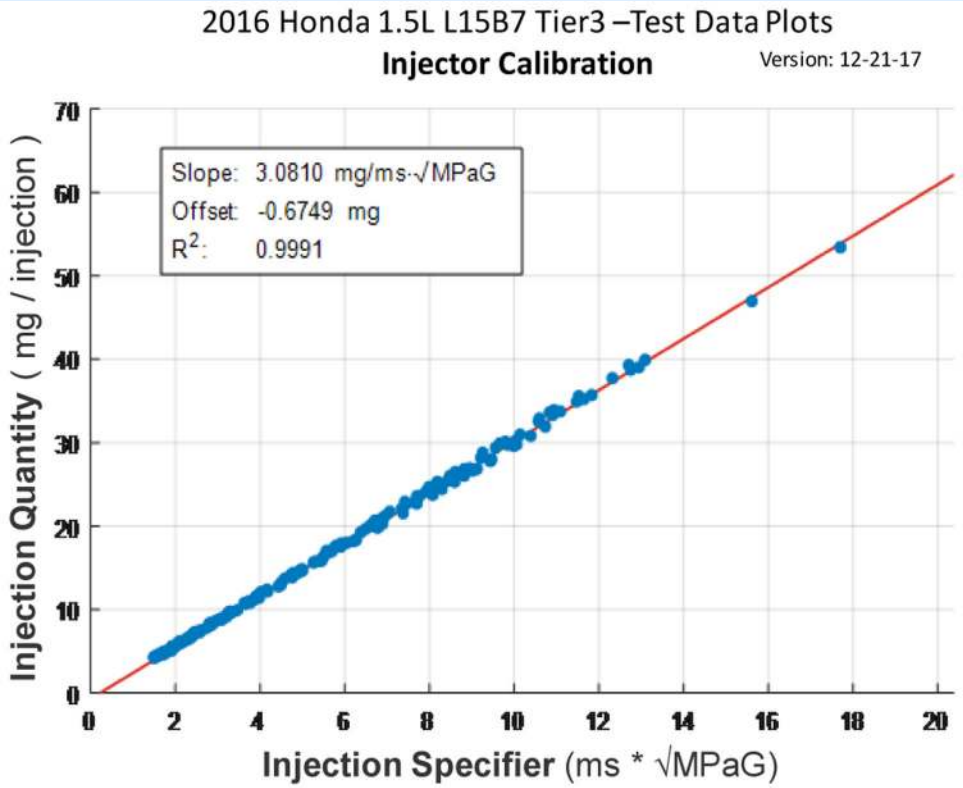

Figure 8.
Injector calibration data

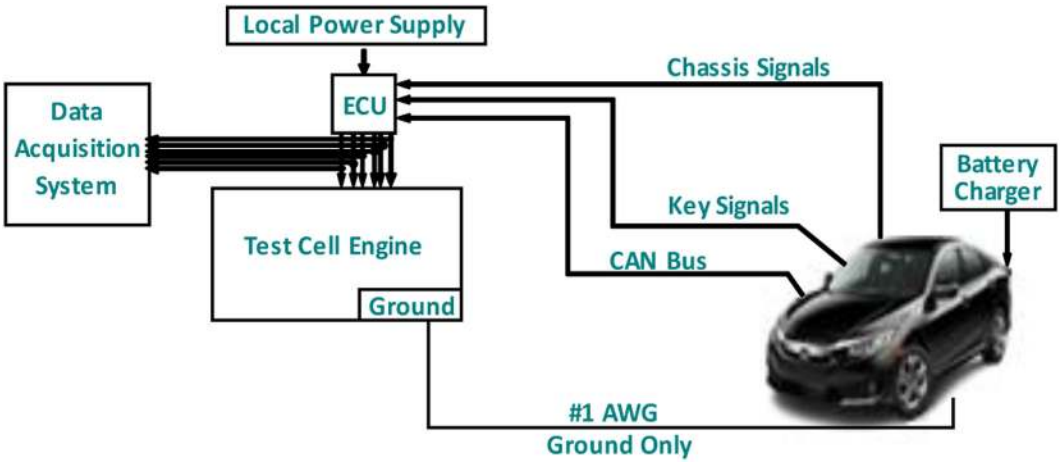

Figure 1.
Vehicle and engine tethered wire harness

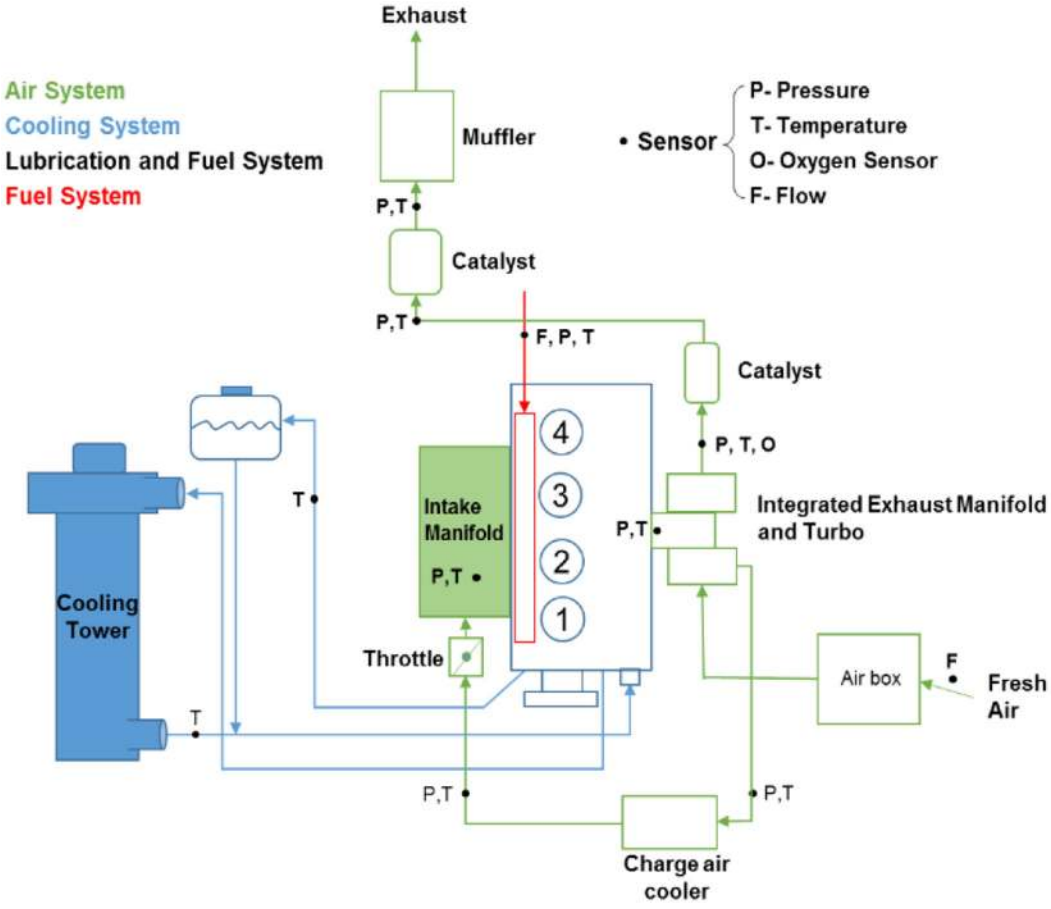

Figure 2:
Schematic of dynamometer test cell and the engine sensor locations corresponding to the identified systems

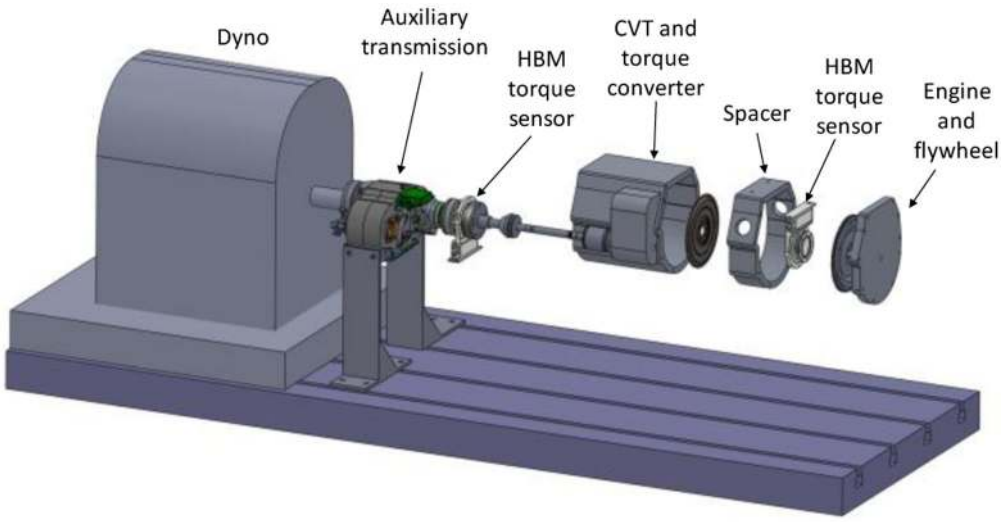

Figure 3.
Engine and CVT setup with torque sensors*

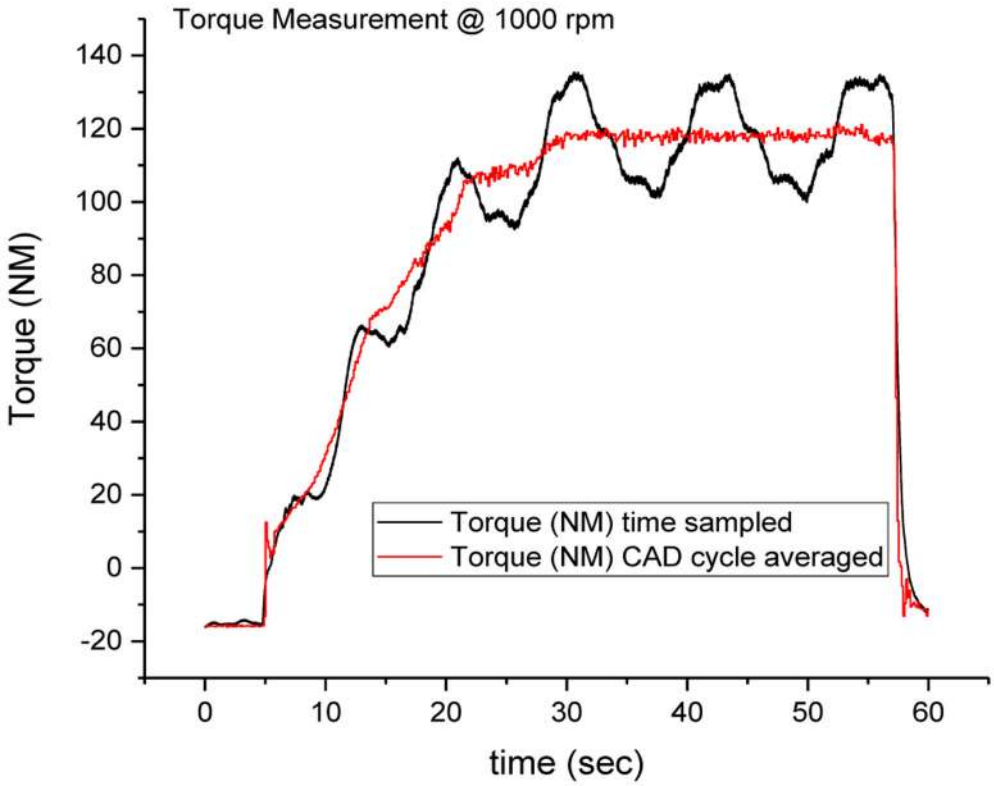

Figure 4.
Engine Torque Measurement Load Sweep

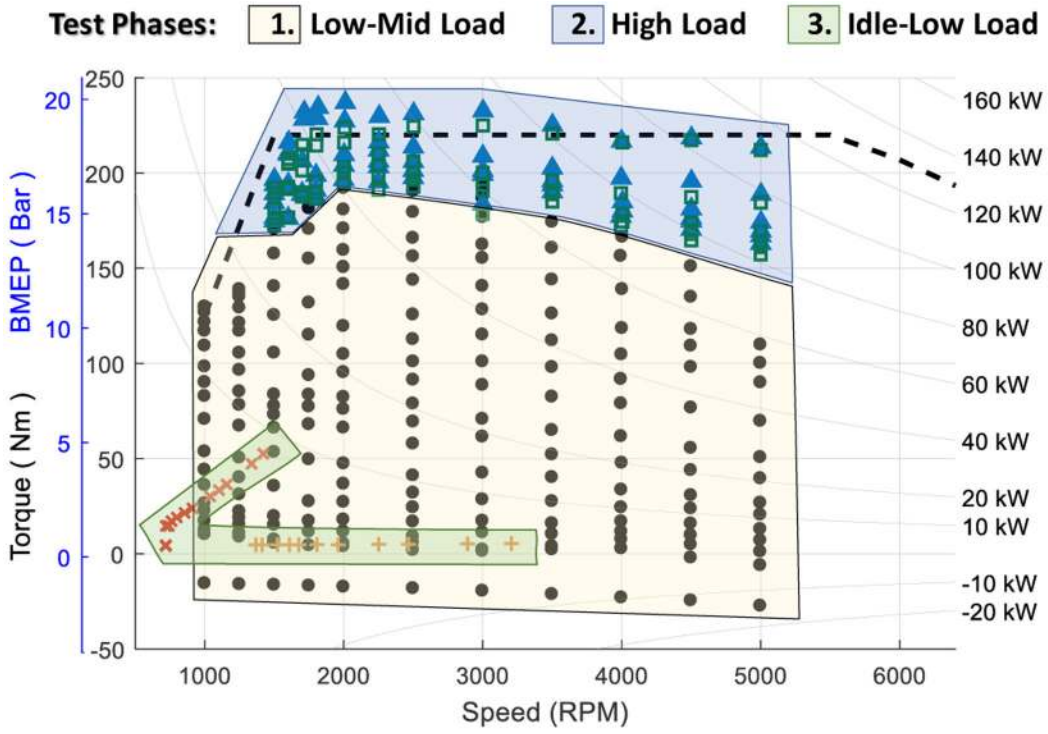

Figure 5.

Engine Mapping Test Data Points from benchmarking 2016 Honda 1.5-liter L15B7 using Tier 2 Test Fuel

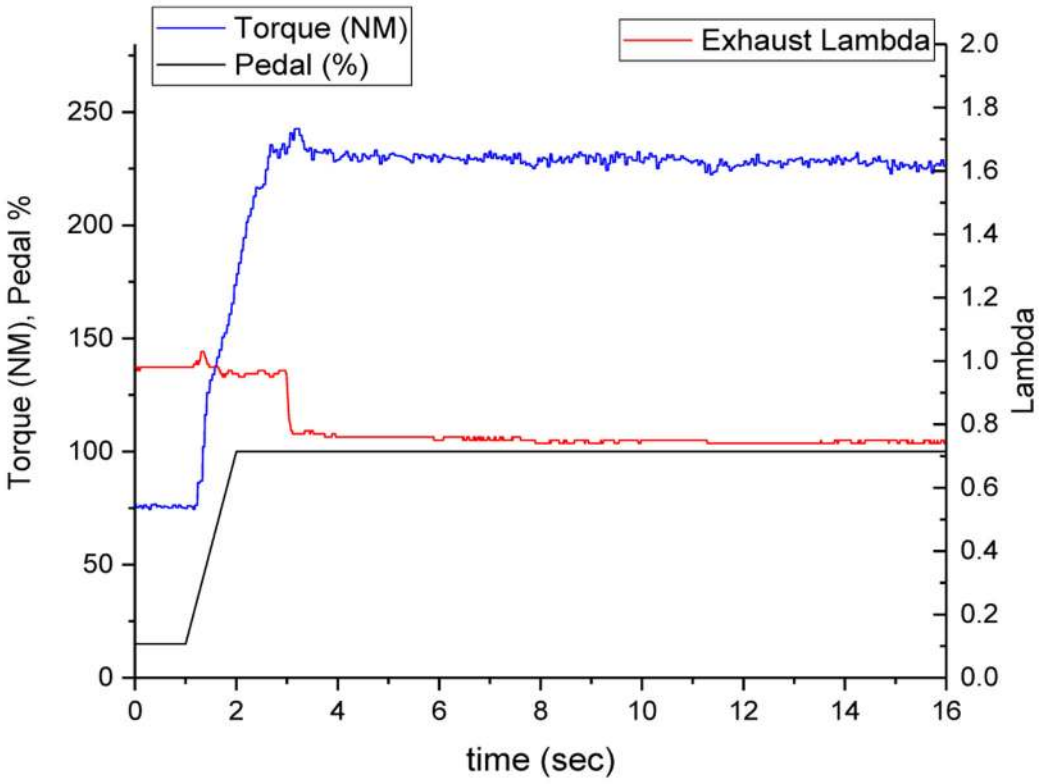

Figure 6.
Example of data collected during Transient test

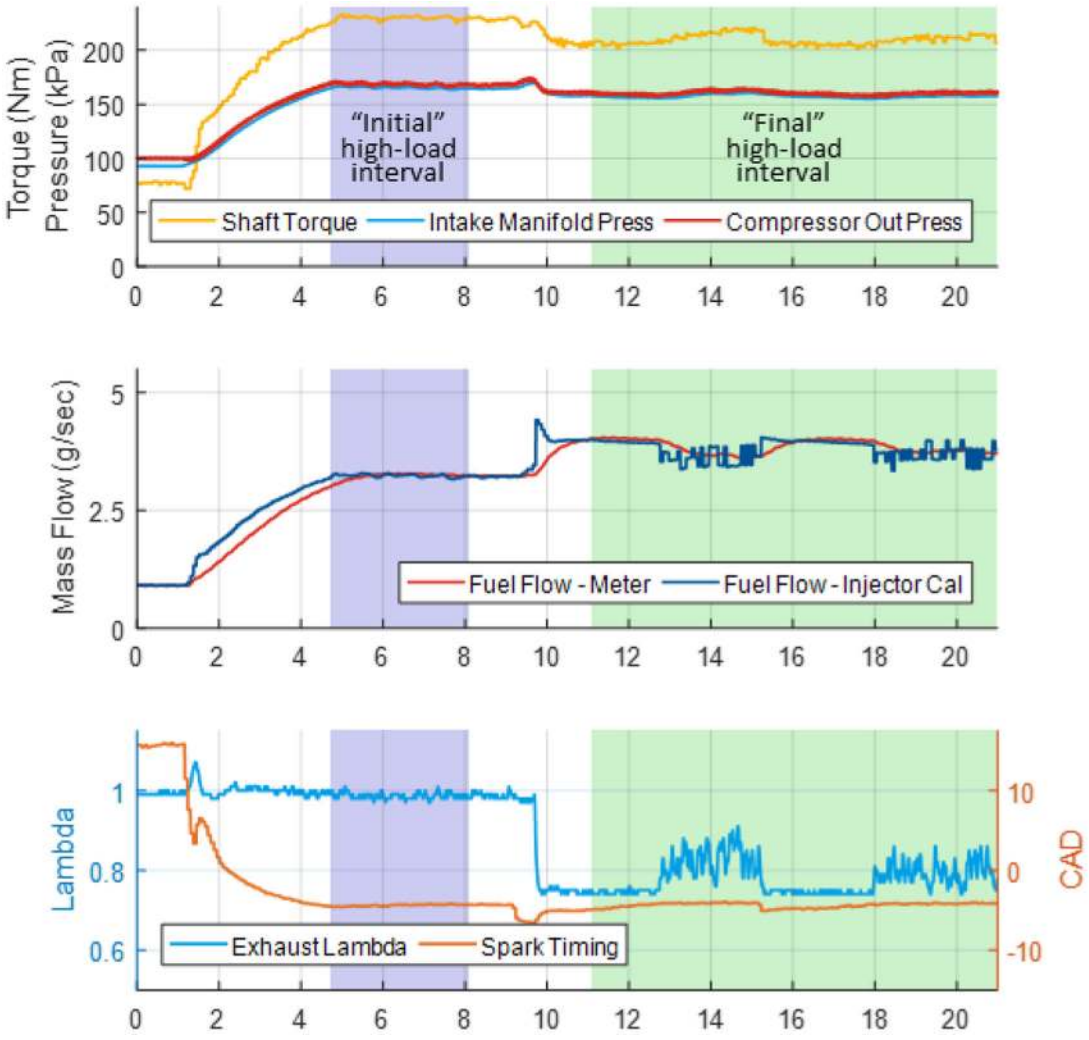

Figure 7.

Example high load test conducted on 2016 Honda L15B7 turbocharged engine showing several pertinent parameters and the windows of data selected.

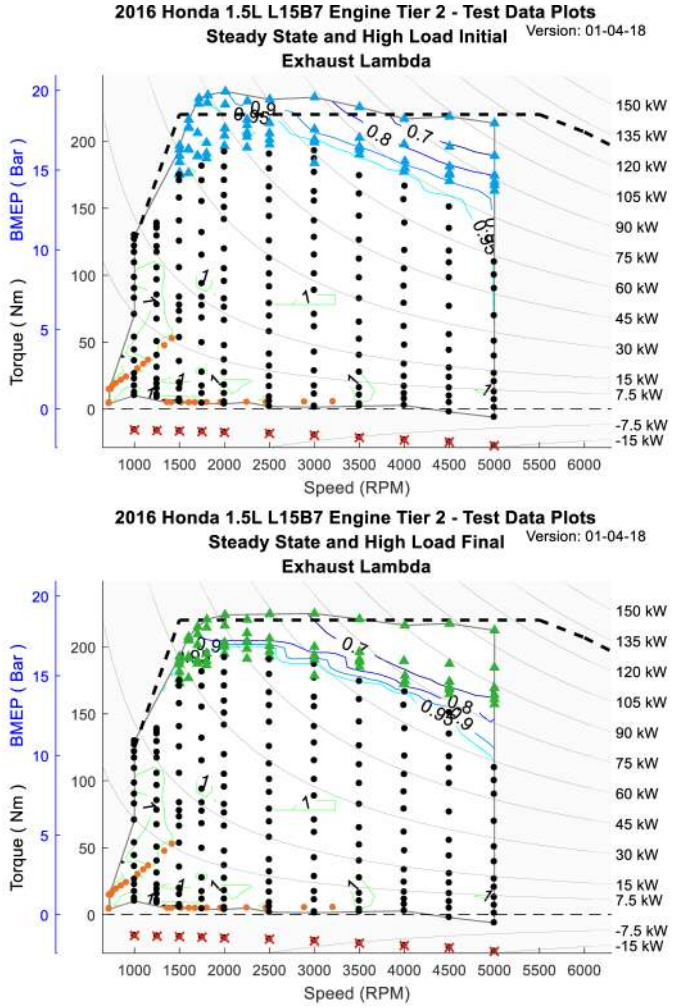

Figure 9.

The Honda 1.5-liter average exhaust lambda in the initial and final intervals of the transient high load data

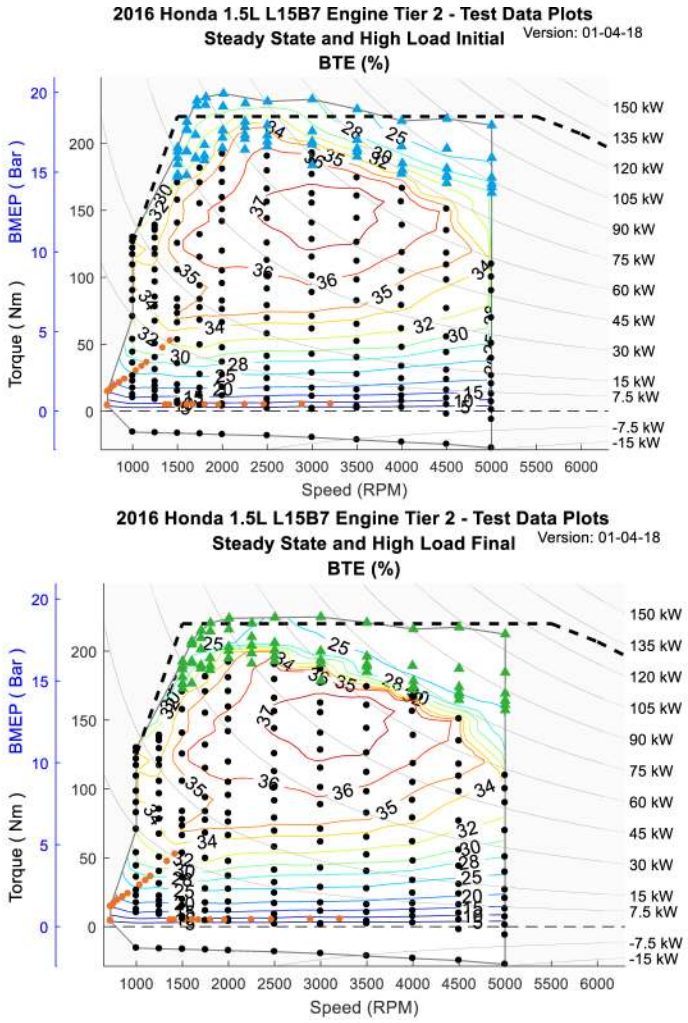

Figure 10.
The Honda 1.5-liter BTE in the initial and final intervals

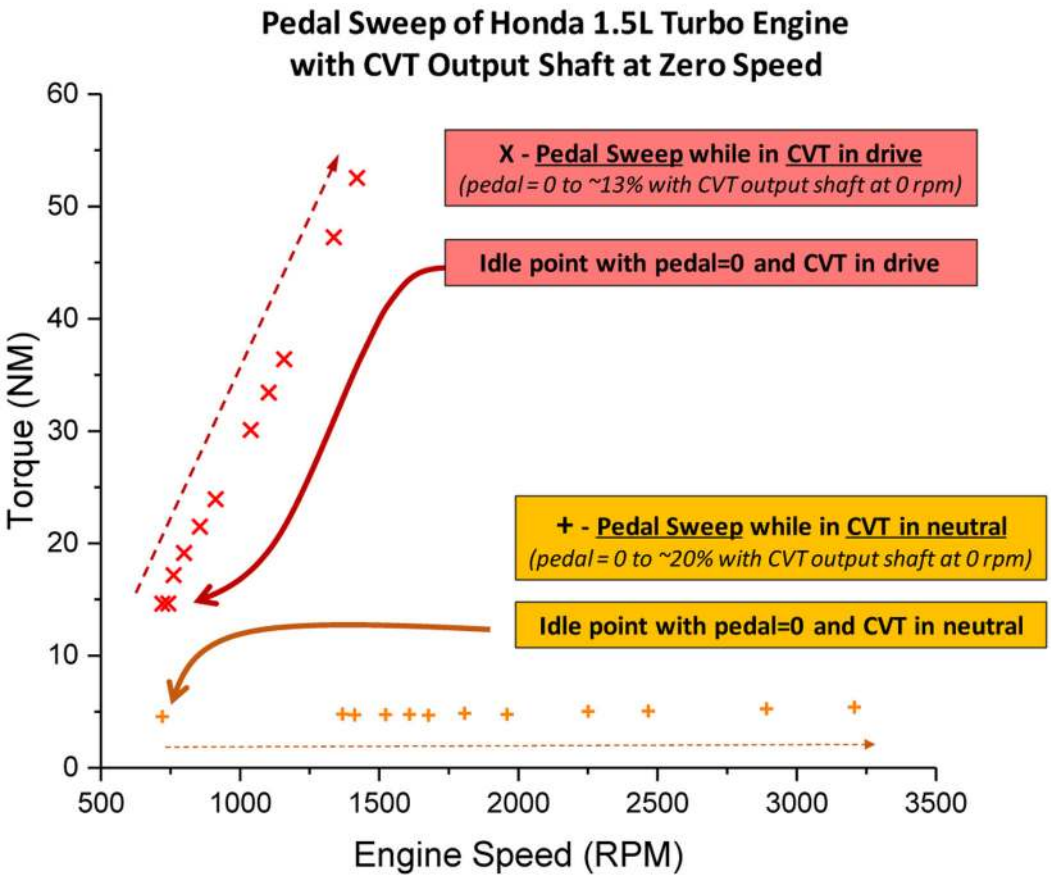

Figure 11.
Test Phase 3 with Idle-Low Loading

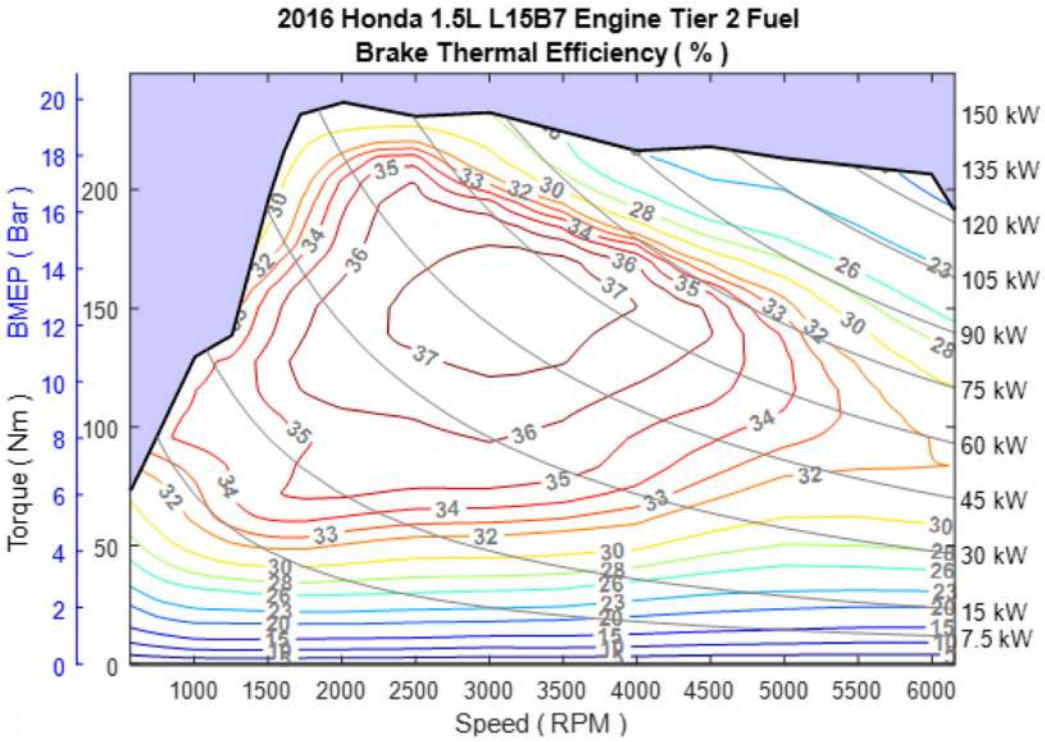

Figure 12.

BTE map generated from EPA test data on the Honda 1.5-liter L15B7 Earth Dreams Turbo – 130 kW, Tier 2 fuel

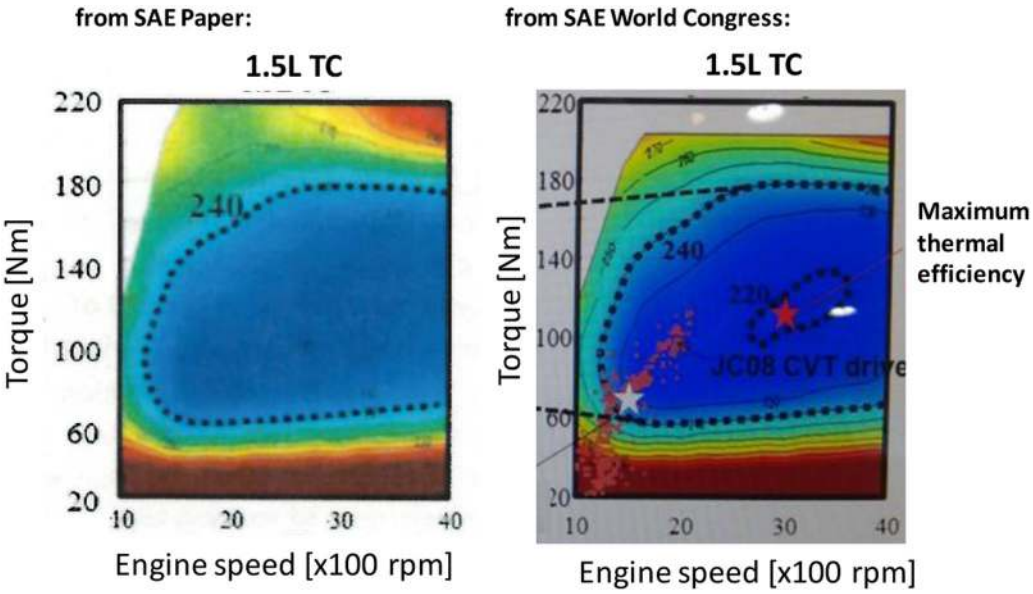

Figure 13.
Honda's two published BSFC maps for its 1.5-liter L15B7 engine

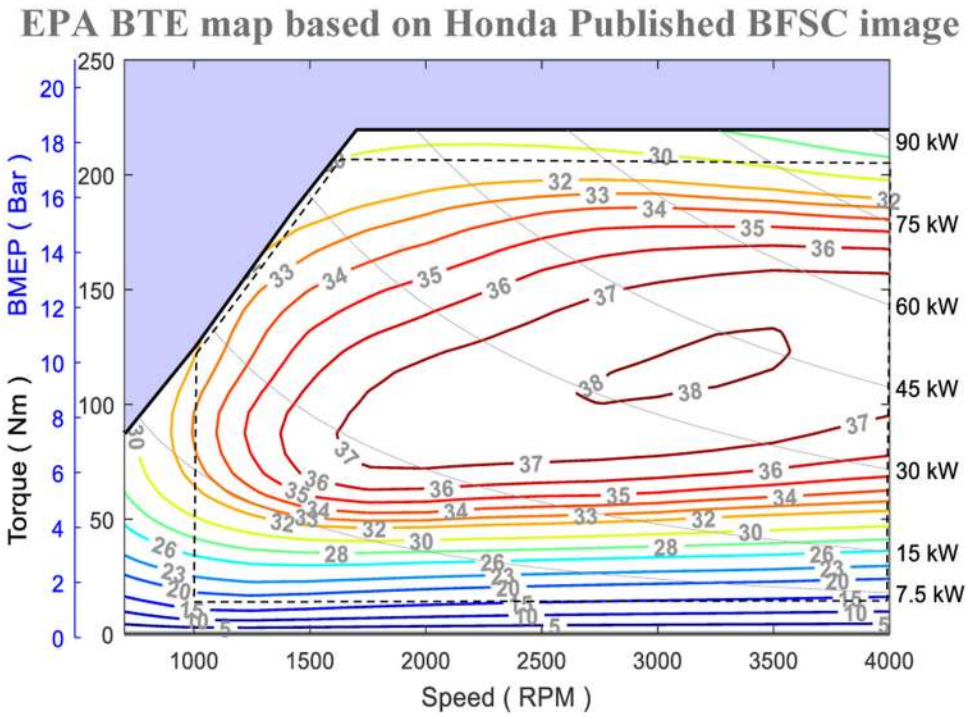

Figure 14.
BTE map generated from the data published by Honda for the 1.5-liter L15B7 Earth Dreams Turbo engine - Tier 2 fuel [3, 4]

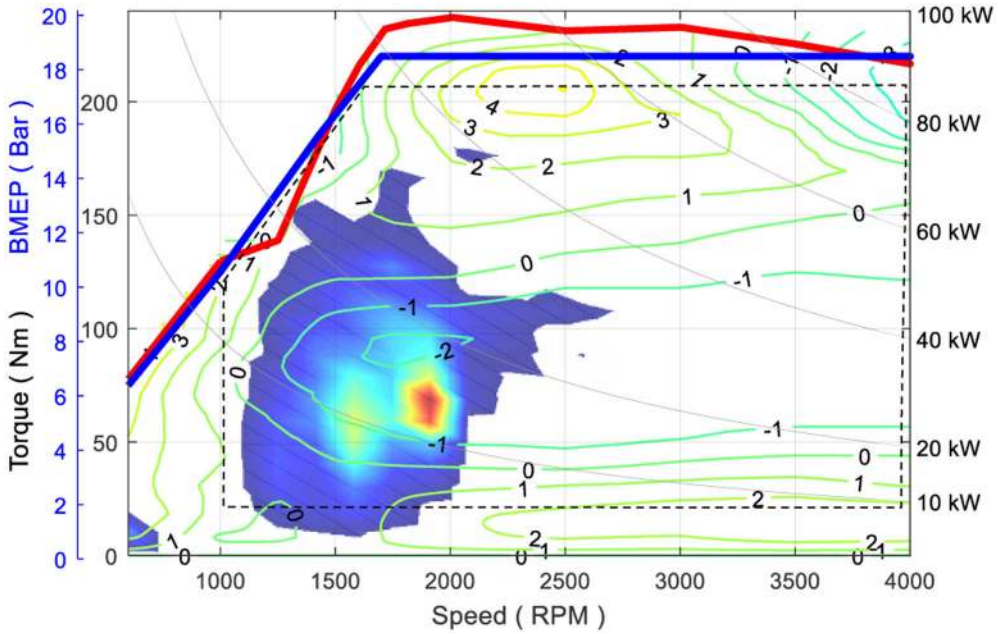

Figure 15. Efficiency (BTE) Difference Plot - Tier 2 fuel
(EPA map from Test Data minus EPA map from Honda published image)

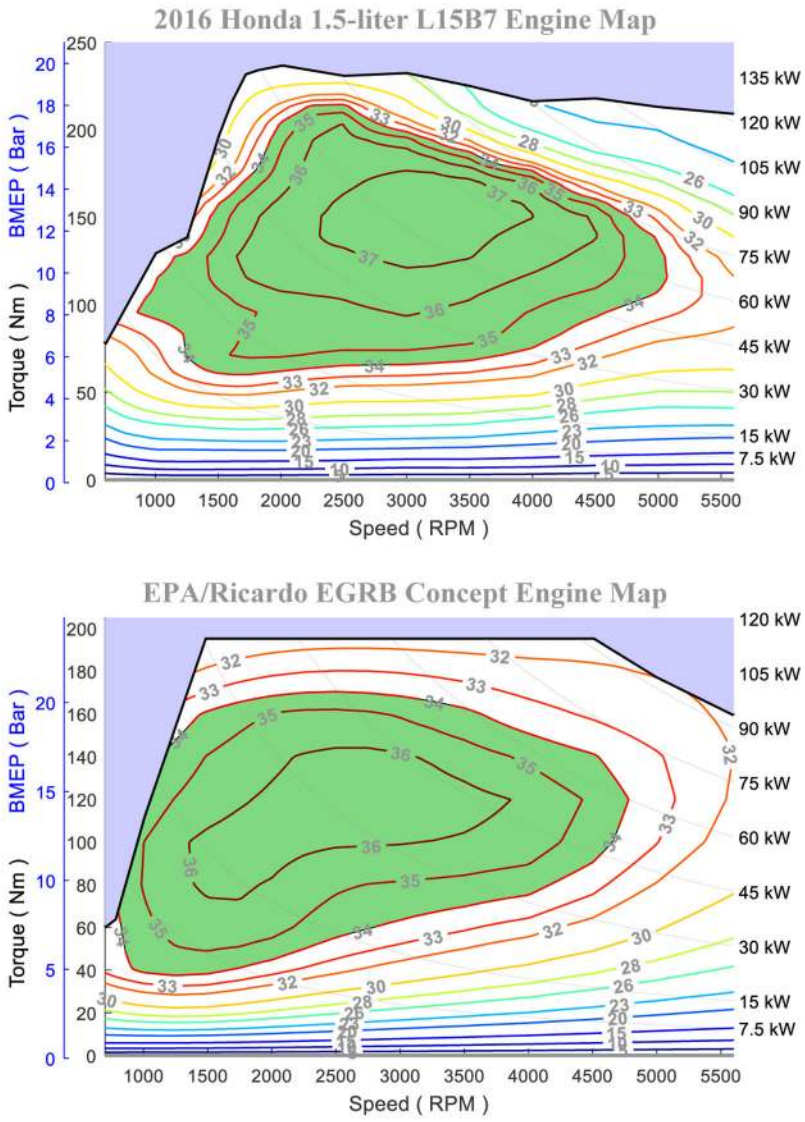

Figure 16:

Comparison of the Honda 1.5L BTE map (top) with the EPA/Ricardo EGRB BTE map (bottom) with green highlighting above 34% engine efficiency

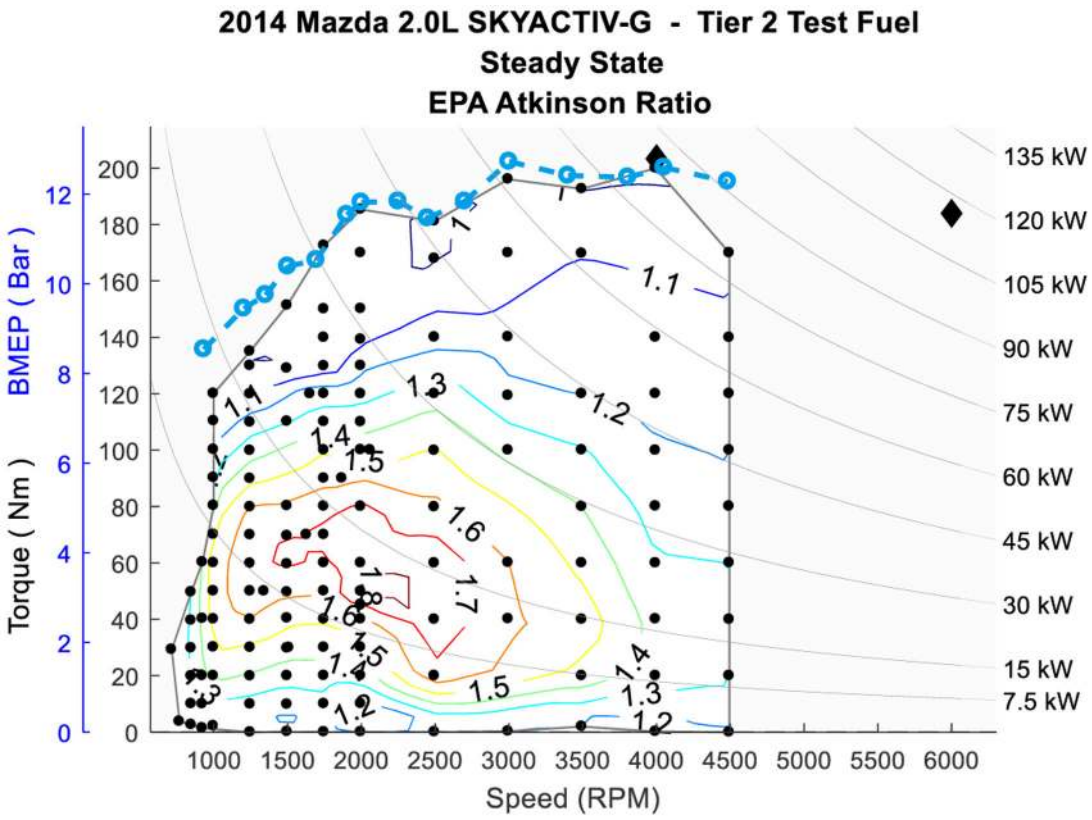

Figure 17.
Atkinson ratio of the 2014 Mazda 2.0 L naturally aspirated engine

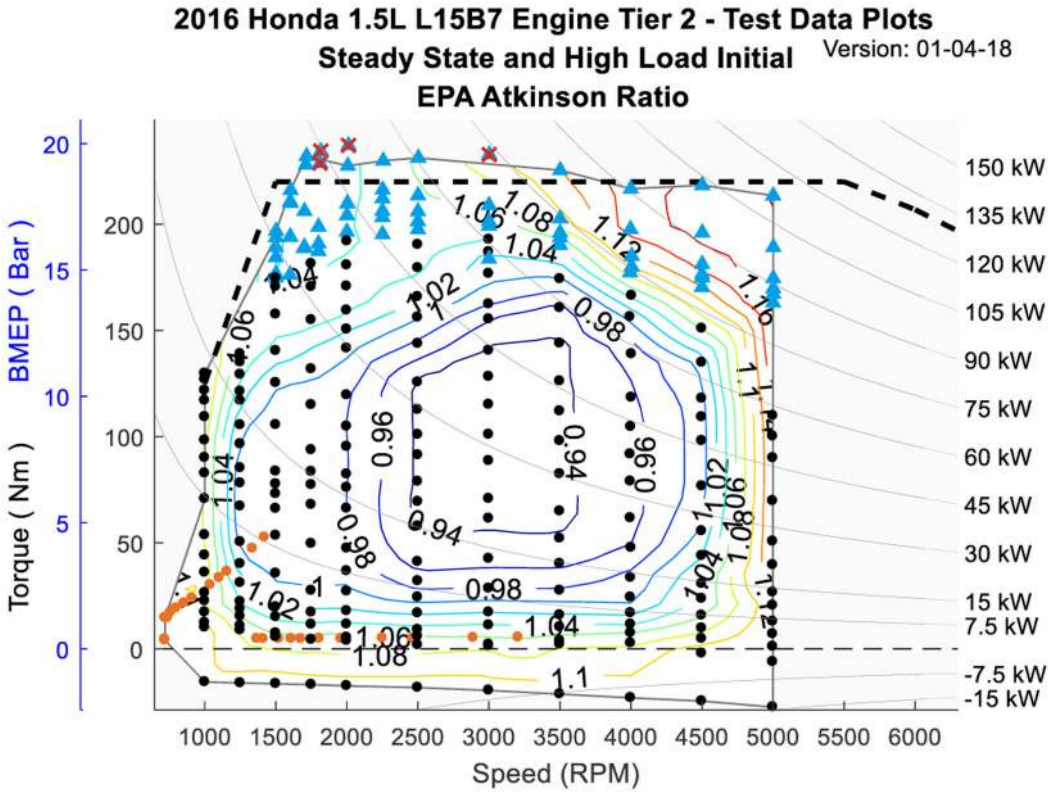

Figure 18.
Atkinson ratio of the 2016 Honda 1.5-liter turbo engine

Table 1:

Summary of Vehicle and Engine Identification Information [3,4]

Vehicle (Year, Make, Model)	2016 Honda Civic
Vehicle Identification Number	19XFC1F9XGE000831
Engine (displacement, name)	1.5-liter, L15B7
Rated Power	174 hp (130 kw) @ 6000 RPM
Rated Torque	162 lb-ft (219 Nm) @ 1700–5500 RPM
Fuel requirement	87 octane Anti-Knock Index (AKI)
Emission level	Tier 3
Advanced engine technology features	• Direct injection • Turbocharger and boosting system • Electronic waste gate actuator • Variable Valve Timing (VVT) • High tumble combustion chamber
Transmission	Continuously Variable Transmission (CVT)

Table 2:

Test Cell Equipment and Instrumentation

Equipment/Instrument Name	Purpose/Measurement Capabilities	Manufacturer
Dynamometer (Alternating Current)	Absorb torque from engine and provide motoring torque to engine	Meidensha Corp., Tokyo, Japan
Torque Sensor	Measure torque	HBM GmbH, Darmstadt, Germany
CVS dilution tunnel	Exhaust flow system	EPA
Coriolis fuel meter	Measure Fuel flow rate	Emerson Micro Motion, St. Louis, MO
Laminar flow element	Measure Air flow rate	Meriam Process Technologies, Cleveland, OH

Table 3:

Engine Control and Data Acquisition Systems

System	Developer	Description	Data Rate
iTest	A&D Technology, Inc., Ann Arbor, MI	Test cell automation hardware and software system that controls the dynamometer and some engine controls; collects test cell data; master data logger.	10–100 Hz
MATLAB	MathWorks, Natick, MA	Software used for development of data processing algorithms for transient testing	--
RPECS	Southwest Research Institute, San Antonio, TX	Crank angle based engine control and data acquisition system that collects ECU analog and CAN data, TCU analog and CAN data, and controls torque converter lock up solenoid.	1/engine cycle

Table 4:

Test Cell Fuel Specifications

	EPA Tier 2 Certification Fuel	EPA Tier 3 Certification Fuel
Fuel Grade	**Premium**	**Regular**
Ethanol Content (%vol.) ASTM D5599	0%	10%
LHV (MJ/kg) ASTM D240	42.898	41.817
Specific Gravity@60°F ASTM D4052	0.74301	0.74850
Carbon Weight Fraction ASTM D3343	0.8665	0.8267

Table 5:

Summary of the engine benchmarking methods and procedures

Test Phase	Engine Operation	Data Collection	Data Processing
1 Low-Mid loading	Approx. 30 sec. (stoichiometric)	Steady-state (wo/CVT)	Steady-state avg. (using iTest)
2 High loading	Stab test (stoich. → enriched)	Transient (wo/CVT)	Transient Intervals (using MATLAB)
3 Idle-Low loading	Approx. 30 sec. (stoichiometric)	Steady-state (with CVT)	Stead-state avg. (using iTest)

Table 6:

Comparison of CO_2 results using EPA's benchmark-based map versus using Honda's published map on a 2016 vintage mid-sized car

Table 6 Part A: ALPHA vehicle simulation results

Veh. Tech.	Engine	Sized Displ. (liters)	Combined Cycle Fuel Economy (MPG)	Combined Cycle CO_2 (gCO_2/mi)	**Map:** % CO_2 Delta (EPA/Honda - 1)	**Year:** % CO_2 Delta (2025/2016 - 1)
	Baseline 2016 mid-sized car	2.437 (I4)	36.8	241.4	--	--
2016	Honda L15B7 Earth Dreams Turbo (map from Honda published image)	1.653 (I4)	39.0	227.8	1.1%	--
	2016 Honda L15B7 Turbo (map from EPA test data)	1.654 (I4)	38.6	230.4		--
2025	Honda L15B7 Earth Dreams Turbo (map from Honda published image)	1.427 (I4)	52.6	168.9	0.9%	-26%
	2016 Honda L15B7 Turbo (map from EPA test data)	1.420 (I4)	52.2	170.4		-26%

Table 6 Part B: Characteristics of 2016 and 2025 mid-sized vehicles

Vehicle Tech.	Transmission	Test Weight (lbs)	Road Load A Coefficient (lbf)	Road Load B Coefficient (lbf/mph)	Road Load C Coefficient (lbf/mph2)	Curb Weight Reduction (%)	Aerodynamic Drag Improvement (%)	Coeff. of Rolling Resistance Improvement (%)	Start Stop	Accessory
2016	6-spd	3510	30.62	-0.0199	0.01954	0%	0%	0%	no	electric_ HPS
2025	future 8-spd	3269	24.74	-0.0199	0.01759	7.5%	10%	10%	yes	electric_EPS_ HEA_REGEN

Table 7:

ALPHA simulations using current production turbocharged engines

Boosted Engine	2016 Sized Displ. (liters)	2016 Combined Cycle Engine Efficiency (%)	2016 Combined Cycle CO_2 (gCO_2/mi)	2016 CO_2 Reduction from Honda L14B7 (%)	2025 Sized Displ. (liters)	2025 Combined Cycle Engine Efficiency (%)	2025 Combined Cycle CO_2 (gCO_2/mi)	2025 CO_2 Reduction from Honda L14B7 (%)
Ford EcoBoost 1.6L	1.688 (I4)	26.0%	247.3	--	1.455 (I4)	26.6%	183.4	--
Ford EcoBoost 2.7L	1.480 (I4)	27.0%	242.7	-1.9%	1.291 (I3)	27.5%	178.5	-2.7%
Honda L15B7 1.5L	**1.654 (I4)**	**27.8%**	**230.4**	**-6.8%**	**1.420 (I4)**	**28.6%**	**170.4**	**-7.1%**

Table 8:

Summary of turbocharged engine specifications

Boosted Engines	Intro Year	US or Euro Calib	Compression Ratio	Swept Displacement (L)	Fuel (Reg/Prem)	Max Power (KW)	Max Torque (NM)	Power Dens. (kW/l)	Stroke/Bore	Oil Viscosity	Intake Cam Phaser Auth (°)	Peak Eff. (on Tier2)
Ford EcoBoost 1.6L	2010	US	10.0	1.6	Reg	146	273	92	1.03	5w20	45	35
Ford EcoBoost 2.7L	2015	US	10.0	2.7	Reg	242	508	90	1.00	5w30	56	36
Honda L15B7 1.5L	**2016**	**US**	**10.6**	**1.5**	**Reg**	**130**	**230**	**87**	**1.22**	**0w20**	**60**	**38**
Mazda SKYACTIV-G 2.5L	2016	US	10.5	2.5	Reg	169	420	68	1.12	5w30	75	?[3]
VW EA888-3B 2.0L	2018	US	11.7	2.0	Reg	137	300	68	1.12	0w20	50-70 ?[3]	37
VW EA211 EVO 1.5L	2019	US	12.5	1.5	Reg	96	200	64	1.15	0w20	70	37
VW/Audi EA839 3.0L V6	2018	US	11.2	3.0	Prem	260	500	87	1.05	?[3]	50	37
Nissan MR20 DDT VCR 2.1L	2018	US	8-14	2.1	Reg	200	390	95.88	1.12	?[3]	50-70 ?[3]	~40% ?[3]
Mazda SKYACTIV-X SPCCI 2.0L SC[1]	2019	US	18.0	2.0	reg	141	280	71	1.09	?[3]	70+ ?[3]	44
EPA/Ricardo EGRB24 1.2L[2]	**N/A**	**US**	**10.5**	**1.2**	**Reg**	**114**	**220**	**99**	**0.96**	**?[3]**	**50**	**37**

1- Supercharged **2**- EPA Draft TAR **3**- Not known at time of writing

Table 9:

Technology content and degree of implementation

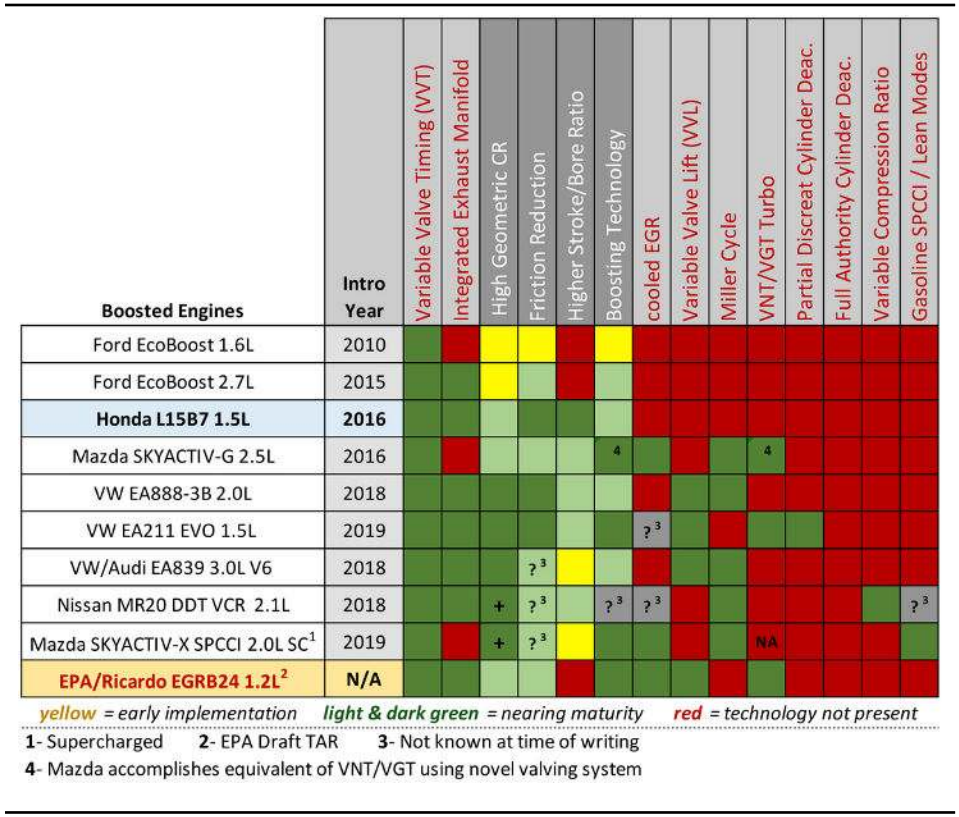

Boosted Engines	Intro Year	Variable Valve Timing (VVT)	Integrated Exhaust Manifold	High Geometric CR	Friction Reduction	Higher Stroke/Bore Ratio	Boosting Technology	cooled EGR	Variable Valve Lift (VVL)	Miller Cycle	VNT/VGT Turbo	Partial Discreat Cylinder Deac.	Full Authority Cylinder Deac.	Variable Compression Ratio	Gasoline SPCCI / Lean Modes
Ford EcoBoost 1.6L	2010														
Ford EcoBoost 2.7L	2015														
Honda L15B7 1.5L	**2016**														
Mazda SKYACTIV-G 2.5L	2016						4				4				
VW EA888-3B 2.0L	2018														
VW EA211 EVO 1.5L	2019							?[3]							
VW/Audi EA839 3.0L V6	2018				?[3]										
Nissan MR20 DDT VCR 2.1L	2018			+	?[3]		?[3]	?[3]							?[3]
Mazda SKYACTIV-X SPCCI 2.0L SC[1]	2019			+	?[3]						NA				
EPA/Ricardo EGRB24 1.2L[2]	**N/A**														

yellow = early implementation *light & dark green* = nearing maturity *red* = technology not present

1- Supercharged **2**- EPA Draft TAR **3**- Not known at time of writing

4- Mazda accomplishes equivalent of VNT/VGT using novel valving system

Table 10:

ALPHA vehicle simulations of current and potential future turbocharged engine technology

Boosted Engines	Sized Displ. (liters)	Combined Cycle Engine Efficiency (%)	Combined Cycle CO_2 (gCO_2/mi)	CO_2 Reduction from Honda L14B7 (%)	Sized Displ. (liters)	Combined Cycle Engine Efficiency (%)	Combined Cycle CO_2 (gCO_2/mi)	CO_2 Reduction from Honda L14B7 (%)
	2016				2025			
Honda L15B7	1.654 (I4)	27.8%	230.5	--	1.420 (I4)	28.6%	170.4	--
Honda L15B7 w/deacFC[1] (est)	1.654 (I4)	28.5%	224.7	-2.5%	1.420 (I4)	29.4%	166.0	-2.6%
EPA/Ricardo EGRB24 1.2L[2]	1.421 (I4)	29.4%	223.3	-3.1%	1.250 (I3)	30.5%	160.8	-5.6%

1- with Full Continuous cylinder deactivation (deacFC) *2- EPA Draft TAR*